MINISTER OF EDUCATION AND RESEARCH
University POLITEHNICA of Bucharest
Doctoral School of Industrial Engineering and Robotics

Oana-Maria D. MANTA (BĂLAȘ)

Research on development of slosh noise baffles for automotive fuel tanks

*** Summary of doctoral thesis ***

Scientific coordinator,
Prof.univ.dr.ing. Cristian Vasile DOICIN

- 2021 -

Content

Forward

Here we are at the end, after several years of doctoral studies. A period full of enthusiasm, challenges, ascents, expectations, results, satisfactions, reflections, understanding, visions, discovered, consolidated, new and old perfected professional and personal skills. Through this professional stage I understand that doctoral studies not only mean scientific input in a particular academic segment, but above all means resilience, communication, tenacity, perseverance, ambition, result orientation, self-leadership, that in the end, the process itself contributes decisively, to my professional and personal definition. Therefore, the completion of this doctoral thesis would not have been possible without the support, support and perseverance of a large collective which I would like to mention in the following.

Thanks to:

Scientific coordinator, Prof. Univ. Dr. Ing. Cristian Vasile Dodicin, who believed in the potential of the doctoral theme and accepted the coordination of this thesis. Transposing my professional achievements into an academic context, the professor being directly involved in all aspects of the work, open communication on potential approaches, advice, targeting, effective support for participation in multiple conferences, drafting of articles, materializing ideas into physical prototypes by 3D printing the necessary elements within the 3D Printing Laboratory of the Faculty of Industrial Engineering and Robotics , are only a small part of the multitude of actions on which he has made his mark and led to remarkable progress in the doctoral thesis. Understanding has been the key to the whole process of these years of doctoral studies.

Lecturer Univ. Dr. Elena Corina Cipu, from the Department of Applied Mathematics of the University Politehnica of Bucharest, for opening, involvement, dedication and support in discovering the links between the movement of fuel in a vehicle tank, the dynamics of the car and the sound perceived by the car user, the end result, the dependencies highlighted by the motion equations having a character of novelty worldwide.

Mr. Eng. Radu Bălaş – Manager Lean 6 Sigma & Digitization at Garrett Advancing Motion Romania, my husband, for his support on statistical interpretation of data, elaboration of testing methodologies, performance of physical tests and last but not least active participation in scientific activities.

The management team of Renault Technologie Roumanie – Mr. Costin Ionescu, Ovidiu Mantali, Gheorghe Marin for the support and resources provided in the design of technical solutions. I have been employed by Renault Technologie Romania since 2012.

Mr. Ing. Ion Comănescu – Director of Platform Engineering at Renault Technologie Roumanie, for patent approval and permission to use technical solutions for academic purposes. The doctoral theme was initiated in a practical, business context, which resulted in six official patents applied and financed by Renault S.A.S. & Renault Technologie Romania.

Mrs. Dr. Anda Dumitrascu - Head of Radiology and Medical Imaging Department, Doctor of Medicine - Head of Laboratory Radiology and Medical Imaging, National Institute of Endocrinology "C.I. Parhon" Bucharest, Audit Team Leader, Quality Management System and Senior HR Consultant, my mother, for support on change management, soft skills, emotional resilience.

Mr. Eng. Dan Manta – General Manager at SC. TAVI COM PROD SERV SRL, my father, for providing the fixed assets necessary to carry out physical tests, namely the test track, the space for creation of the test laboratory as well as supporting means for carrying out activities in optimal conditions.

The years pass quickly, and I seem to have evolved even faster from one status to another, reaching today to be the mother of two wonderful boys (Stefan and Dimitri), employee of the Renault group for nine years, doctoral student, but also wife, daughter, niece, active in their duties. None of the above would have been possible without the unconditional support of my husband, my mother and my grandparents who made sure that my professional development was perfectly integrated into the harmony of family life. Together we are a team. Thank you so much, my beloved family!

Introduction

The doctoral thesis entitled "Research on development of slosh noise baffles for automotive fuel tanks " presents the research undertaken by the author on the achievement of the objective of the paper, of shaping the dynamic behavior of the fuel in the car tank during their movement and on the development of innovative technical solutions of integrated wave breakers baffles-also adaptable to existing fuel tanks , in order to improve the phenomenon of slosh noise.

The doctoral thesis aims to come up with solutions to improve the noises produced by the phenomenon of blinking, also known as the phenomenon of "slosh noise", which occurs when the fuel hits the walls of the tank of the car in which it is stored. The work is structured in eight chapters, starting with the presentation of an overview of the current market of cars and fuels used, as well as future trends from the perspective of the fuel system, and then to detail the development of technical solutions aimed for reducing the slosh noise effect, shaping the dynamic behavior of the liquid in the tank , designing anti-flashing systems, then improving the proposed solutions and validating the results obtained.

The first two chapters provide a working basis for the analysis of current solutions and the development of new concepts necessary due to the progress of technology, safety regulations, pollution rules, market requirements, continuous improvement and cost reduction policy in the industry, as well as customer needs.

The third chapter, "The objectives of the doctoral thesis", defines the main objective of the thesis: "*Development and implementation of innovative wave breaking systems, integrable in the envelope of an existing fuel tank, so as to modify the dynamic fuel behavior of the liquid and to reduce the slosh noise phenomenon",* as well as the objectives derived from the work, so that the problem identified above passes into the effective resolution phase by applying technical solutions with industrial application and proven efficacy, through actual physical tests based on prototype components.

Chapter Iv, "Theoretical and practical contributions to the development of anti-slosh noise systems for motor vehicle tanks" , proposes three technical solutions for reducing slosh noises, which are based on the boarding or, more specifically, the integration of "wings" elements on a part already existing inside the tank, namely, the delivery pump module. Therefore, it passes from the drafting stage of the technical solutions of wave breakers on the delivery pump module, to advanced conceptual design and like this, the first step is taken to demonstrate industrial applicability.

Chapter five, "Static analysis of variants of slosh noise reduction systems developed" makes the transition from advanced design to testing of the three technical solutions studied through numerical simulations.

Chapter six, "Dynamic analysis by mathematical modeling of the movement of fuel waves in a tank, with and without slosh noise baffles" presents the transposition of the phenomenon of slosh noise into mathematical language by moving free surfaces in two contexts, in a tank without a baffle compared to a tank presenting wave baffles solutions.

Mathematical modelling of phenomena revealed a softening of the waves and, by implication, the noise caused by them, which was also demonstrated by the use of new models of wave breakers – consisting the subject of national and international patents. It was pointed out that the implementation of a technical solution to break the waves reduces the amplitude of the movement of the free surface of the fuel in the tank by half.

Chapter seven, "Functional analysis - acoustic tests on the use of variants of slosh noise reduction systems under real conditions" begins with the physical realization of all the components necessary for a test, under real running conditions. As there is currently no standard test procedure for reproduction of

the "slosh noise" phenomenon, the vehicle equipped with the test bench, the associated instrumentation and the parts subject to testing has run according to author's own test methodology, defined in accordance with the literature, which allows the reproduction of waves under conditions that a customer may encounter during urban conditions driving. The recorded data were filtered, statistically analyzed and interpreted.

The eighth chapter, "General conclusions, personal contributions, dissemination of results, future research directions", incorporates the conclusions at each stage of the research carried out, to finally confirm the main objective of the thesis. The novelty level of the studied solutions, the inventive activity, the numerical simulations, the mathematical modeling and the physical tests that confirmed their industrial applicability, allowed the patenting of the ideas retained, the author being the holder of a national patent, four international patents and six patent applications on the topic addressed in the present paper. Articles related to the literature have also been published. In addition, further research directions have been identified.

Glossary of terms

CAFE	Corporate Average Fuel Economy
CAGR	Compound growth rate
CAN	Controller Area Network
ECV	Electrical Charging Vehicle
EMAG	Methyl ethers of fatty acids (Esters méthyliques d'acides gras)
EPA	Environmental Protection Agency
EU27+2	European Union (27 states) plus Switzerland and Norway
FDM	Fused Deposition Technology
GDI	Gasoline Direct Injection
GHG	Greenhouse gas
GNC	Compressed natural gas
GPL	Liquefied petroleum gas
HAP	Polycyclic aromatic hydrocarbons
HDPE	High Density Polietilene
HEV	Hybrid Electric Vehicle
MA	Analytical mathematical model
MJP	Fuel delivery pump
MN	Mathematical numerical model
NVH	Noise, Vibration and Harshness
PE	polyethylene
ROV	Roll Over Valve
TFT	Thin-film-transistor
UE	European Union
WWFC	Worldwide Fuel Charter

List of standards:

Nr.crt.	Cod	Description	Content
1.	EN228	Carburants pour automobiles - Essence sans plomb - Exigences et méthodes d'essai	Requirements and test methods for unleaded petrol fuels
2.	EN590	GAZOLE	Physico-chemical properties for diesel

1st Part: State of the art of research on fuel behavior inside an automotive fuel tank and the existence of slosh noise baffles systems

CHAPTER 1: State of the art of research on fuel behavior in the vehicle tank and the development of slosh noise baffles systems

1.1. Fuel tank system

Forty years ago, vehicle fuel tanks were made of metal. However, although they provided an excellent barrier against pollutant emissions, they faced problems due to corrosion, lack of tightness and high mass. Because of these considerations, the automotive industry has started to look for alternatives and turn to plastics [ALV96]. Thus, in Europe 1976 was manufactured the first plastic fuel tank (HDPE mono layer). Its success was based on corrosion resistance, low mass, impact resistance, geometric flexibility, easy production system, environment and much improved working conditions[1] [PLA19]. The high share of HDPE plastic-based manufacturing technology is given by the two types of plastic tanks: monolayer and multilayer coextruded (Fig. 1.1). Through durability point of view, the performance of barrier layer presents an incomparable attractivity in comparison with fluorination solutions. [ZOH11].

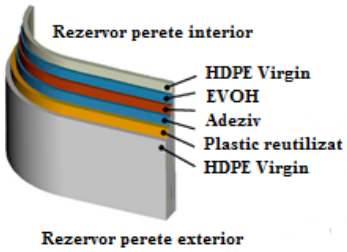

Fig. 1.1. Structure of a multi-layer fuel tank [WAL15]

The fuel tank system (fig.1.2) is characterized by the following main functions: filling, storage, feeding, indication of fuel level. Its constraints are related to regulations, vehicle architecture, acoustic requirements, etc.[AUT14].

In the case of plastic tanks, the main technologies used are: (1) thermo-blowing in the mold – obtaining a fluorinated monolayer tank and (2) blowing coextrusion into the mold – obtaining a multilayered tank. Alternatively, the thermo-blowing of multilayer sheets can be maintained. The advantage of the following is that, together with the blowing of the tank, the pipes/pump module/other accessories are added to the interior, allowing the reduction of connection points and, by implication, leading to the simplification of the manufacturing process, but also to the reduction of the amount of emissions.

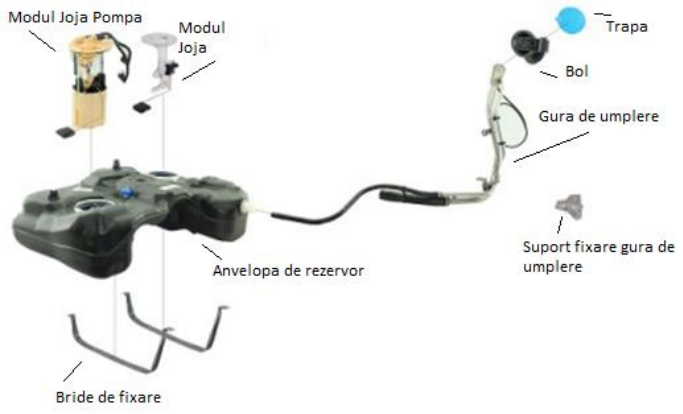

Fig. 1.2. Fuel tank system [A2M15]

The types of technologies used to manufacture plastic fuel tanks influence how solutions can be integrated to mitigate the noise produced by waves inside the tank. Thus, there are geometric solutions integrated in the shape of the tank envelop in the process of blowing into the mold, solutions of breakers welded directly into the envelope during the double blow in the mold (twin sheet blow molding, fig.1.3.), or even slosh noise baffles solutions welded after the process of blown into the mold.

«Fuel is a liquid fuel used in internal combustion engines» [DEX15]. Fuels are substances that react chemically with another substance to produce heat or produce heat through nuclear processes. In Europe there are two main rules: EN228 which defines the quality of petrol and EN590, which defines

[1]Resilient and lightweight plastic that allows manufacturers to significantly reduce vehicle weight, increasing fuel efficiency.

Fig. 1.3. Fuel tank detail of Twin sheet blow molding [PLA16]

the quality of diesel. All existing fuels must comply with the normalized technical specifications underlying the two rules (EN590, EN228) [MAT16]. Horizon 2024 shows the switch to EURO 6/7 and a CAFE coefficient = 95 g/km, Fig.1. 4. In addition, 10% of the energy used in transport will be renewable, in order to maintain the sustainability of biofuels.

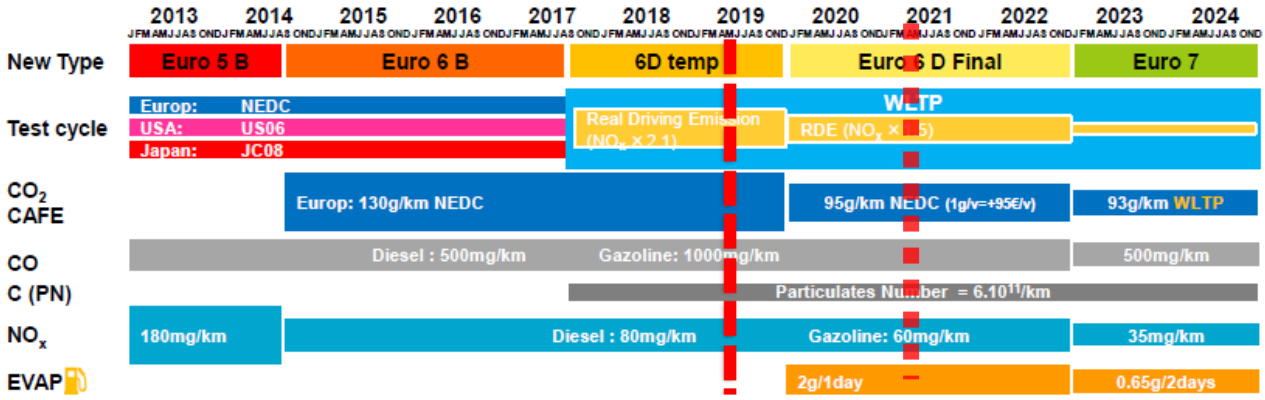

Fig. 1.4 Evolution of Euro rules [IFP16]

1.2. Fuel behavior in the tank

The tank provides several functions: supply, storage, fuel level indication and ventilation. While running, once the fuel from the tank is operated by a delivery pump to supply the engine with the necessary fuel, certain movements of the liquid called waves are produced [HAL11]. When the vehicle is running – by accelerating, deceleration, sudden stopping or by crossing a bumpy road, waves form inside the tank. They end up breaking and hitting the walls of the container. The more the waves have a greater amplitude, the more violent the contact with the wall is. The noise produced by this type of wave is known as "slosh noise". The phenomenon consists, in fact, in the continuous movement of the free surface of a liquid in a partially filled enclosure with noise generation. The moment of inertia exerted by the liquid is strongly correlated with the unit of time and may even be superior to the force of gravity exerted by a solid with similar mass. This is one of the foundations underlying the transport and storage of liquids. The most eloquent example is given by fuel tankers. Due to the dynamic behavior of the liquid transported, it may have a major influence on the road. The situation is encountered in the case of the transport of liquids by sea, rail, etc.

Through the "Problem solving" methodology [ADA16], the most efficient and economical plan of action in this case is to solve the phenomenon by changing the design of the tanks, integrating solutions for breaking the waves. In addition to the multiple advantages associated with this solution, there are negative aspects too, such as the reduction of the useful capacity of the tank and, by implication, the volume of expansion associated with a quantity of fuel, as well as the high price of the technology, must also be taken into account.

The phenomenon is very often encountered at plastic tanks(HDPE). They are lightweight and at the same time resistant. The technology of obtaining them, thermo-blowing in the mold, allows to decrease the thickness of the walls of the tanks, which leads to the amplification of the noise felt in the passenger compartment, produced by the movement of the liquid. This confirms the need of implementation of

complex geometries in order to reduce wave generation or decrease their amplitude. However, the increased efficiency is given by the insertion of wave breakers during the blowing process and beyond. This type of solution poses a real challenge for tank suppliers. The physical result is influenced by the number of inserted wave breakers, their shape and sizing. In addition to acoustic optimization, the tensions at the walls and welding points decrease, thus increasing the life of the product.

Currently, there is no standard procedure, a clear series of parameters that could be defined and applied to resolve the slosh noise effect. The input data is very varied and variable, and the occurrence of waves cannot be transformed into a 100% predictable event.

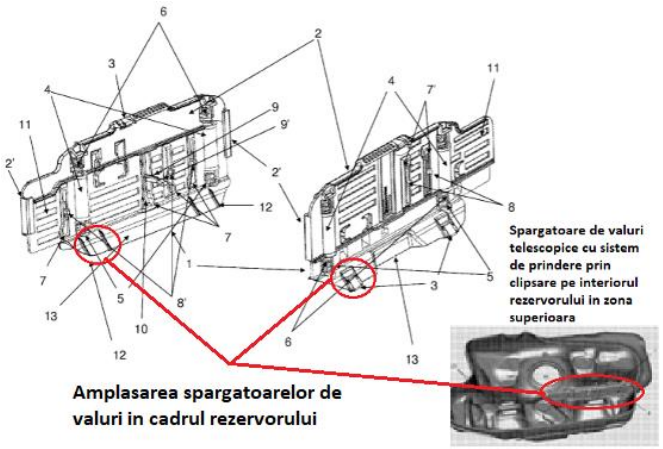

Fig. 1.5. Telescopic breakers [JAC11]

In general, most developed wave breakers are fixed in the tank after blowing it, by insertion through one of the tank openings, such as the fuel pump module insertion hole. Due to the large size of some baffles that could not be inserted through standard openings, Inergy Automotive Systems Research identified the desirability of developing retractable wave breaking baffles(Fig. 1.5).

In order to keep the baffle in position, double fastening zones have been created within the tank envelop, both at the bottom and at the top. The material from which the baffles of this type are made is HDPE. In order to reduce the wave breaker dimensions, as well as to preserve the properties of mechanical strength, both components (upper and lower) have various ribs and cutouts [JAC11].

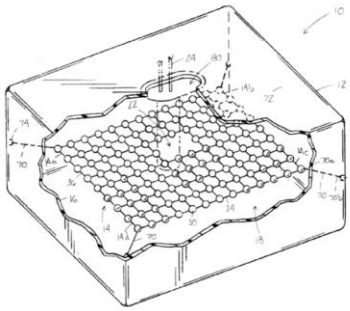

Fig. 1.6. Absorbent net [RAM09]

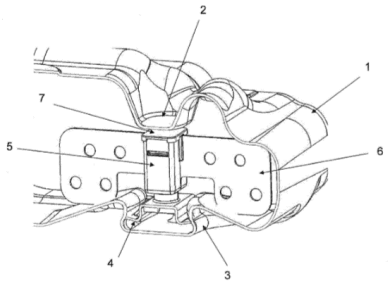

Fig. 1.7. Dual function breaker for negative pressure-resistant tanks [PAR10]

In some countries, due to regulations that impose the implementation of OBD (On Board Diagnostic Systems) rules, it is necessary to test the tightness of the tanks by applying negative pressures. Thus, the tank design comprises sections of interference between the lower surface and the upper surface of the tank. Inergy also uses the shapes created as wave breakers (Fig. 1. 7). As can also be seen in the figure , 1.7, there are also disadvantages in reducing the useful capacity of the tank and increasing its mass [PAR10].

In order to identify technical solutions for wave breakers, a benchmark was developed based on the analysis of 23 models of tanks belonging to vehicles in segment B(details inTab.1.13 of the thesis). The analysis was carried out both by participating in the car disassembly workshops that took place within the Renault Group in Romania and France, and on the basis of the information available in the database "a2mac1". Key characteristics such as: tank mass, size, volume, material and the existence of wave breakers were considered for this study [A2M15]. It was found that out of 23 cases analyzed, only 17.4% had metal tanks with baffle solutions integrated. There are also metal baffles attached to the upper/lower shell by multiple welding points.

Of the remaining 82.6% of plastic tanks, only 8.69% have integrated tanks in the tank envelope. None of the plastic tanks analyzed showed any solution of integrated baffles in the tank (by welding in line or offline).

Car producers have worked with tank suppliers to find various methods of wave reproduction since the tank development phase. They turned this effect into a requirement for the acoustic performance of a tank. Currently, there is no standard procedure, a clear series of parameters that could be defined and applied to resolve the slosh noise effect. Input data are very varied and variable, and the occurrence of waves cannot be transformed into a 100% predictable event[JAC11].

CHAPTER 2: Conclusions on the current state of the research

This first part is an introduction to the automotive field, fuels, tank systems and identified problems. The phenomena that occur inside the tank, such as the movement of fuel and waves generation, highlight the complexity of the overall physico-chemical properties of a liquid, but also the importance of applying technical solutions with high impact.

A notable and important aspect is that there is currently no standard procedure for reproducing wave events and no template for applying a particular technical solution. It is a starting approach that allows for diverse analysis and innovations to be carried out.

Wave breakers/ baffles are the subjects of many patents, but their applicability is still not proven on a global scale. As customer demands increase, materials evolve and noise becomes more and more perceptible by the customer. Wave breakers will be reinvented so that the implementation of such a solution will no longer be confronted with financial difficulties, time or even resource considerations.

Part Two: Theoretical and practical contributions to the development of anti-flashing systems for motor vehicle tanks

CHAPTER 3: Objectives of the doctoral thesis

Based on the analysis of the specific literature on the various types of fuels used, the technical problems they may generate, the slosh noise phenomenon and the behavior of the liquid inside the tank of a vehicle, presented in Chapter 1 on the current state of this thesis, it has been established as the main objective of doctoral scientific research the following:

Development and implementation of innovative wave braking systems integrated into the envelop of an existing fuel tank, in order to modify the dynamic fuel behavior and reduce the slosh noise phenomenon.

In order to achieve the main objective, the following derived objectives have been defined:

a) Research on the development of a wave braking system for motor vehicle tanks:
   - Develop integrated wave breaker concept in an existing fuel tank;
   - Study of technical solutions of wave breakers boarded on the delivery pump mode;
   - Static analysis of the variants of wave braking systems developed by performing numerical simulations in the ANSYS V19.0 Static program for the study of the deformability and breaking resistance of the technical solutions studied;
   - Mathematical modelling for the two hypotheses to be studied: the fuel tank without technical wave breaking solutions and the fuel tank that presents solutions against slosh noise;
   - Correlation of the movement of free surfaces with the noise level generated through the approach of mathematical modeling.

b) Experimental research on functional analysis - acoustic tests based on the use of variants of wave braking systems under real conditions:
   - Elaboration of the test method and scenario to follow;
   - Design and manufacture of the necessary prototypes and needed test support;
   - Determining the limitations of test hypotheses;
   - Conducting actual acoustic tests;
   - Collection of records and filtering of representative data;
   - Statistical analysis of processed data;
   - Dissemination of the results obtained;

In order to accomplish the main objective, as well as the derived objectives, the following activities are carried out:
- Design of generic models for parts of the test assembly;
- Study of optimal materials for the manufacture of wave breakers;
- Identification of the optimal material for 3D printing of prototype parts and its limitations in relation to the material used in the numerical simulations carried out;
- Optimized design for 3D printing of the necessary prototypes;
- Development of a methodology for testing technical solutions by reproducing the internal waves generation in real conditions: on the car within a generic tank;
- Validation of industrial applicability for studied wave breaker technical solutions;
- Validation of the efficiency of innovative technical solutions to reduce the slosh noise effect in relation to an integrated wave-breaker-free tank.

CHAPTER 4: Theoretical and practical contributions to the development of anti-slosh noise systems for motor vehicle tanks

4.1. Design of anti-slosh noise systems for car tanks

Following the benchmark study described in Chapter 1 of the paper, key characteristics were considered, such as: tank mass, dimensions, volume, material and the presence of wave breakers. Thus, the first hypotheses were developed for the development of a generic tank model that will be used for the study of integrated wave breaker solutions.

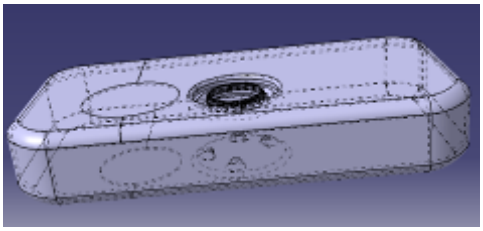

Fig. 4.1. Detail of the generic model of fuel tank

For the choice of the shape regard to the general tank model to be studied, a cuboid e.g. the sides calculated as an average of the tank lengths and size values shown in Table 13 (see detailed thesis)) of Chapter 1 was considered. The width is calculated as the size needed to get the average volume in the study. Therefore, the tank will have dimensions 1000 X 520 X 160 mm. It will respect the particularities of a plastic tank, such as the thickness of the side walls (2-4mm), rounded edges, areas for fixing the Fuel Delivery module (Fig.4.1). Starting from the generic tank obtained, several conceptual variants were made (Fig. 4.2, 4.3) for the further realization of wave-breaker concepts. For the solution shown in Fig. 4.2, the main advantage is that it does not add additional operations to the technological manufacturing process and can be used for several tanks. The disadvantage of such a solution is that it reduces the useful volume of the tank, at the same time, can only be implemented by significantly modifying the current design, but can be considered regarding the situation of the tanks in the design phase.

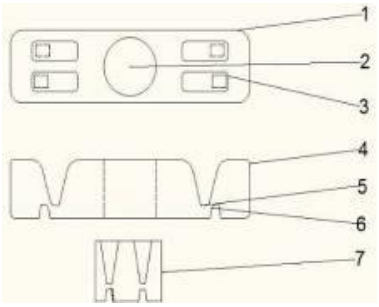

Fig.4.2. Solution A – front view of breakers integrated into the shape of the tank tire during the mold blowing process, both on the lower shell and on the upper shell; 1/top view of the tank; 2/pump mode; 3/top view of the breaker; 4/ front view of the tank; 5/front view of the upper breaker; 6/ front view of the lower breaker; 7/ side view

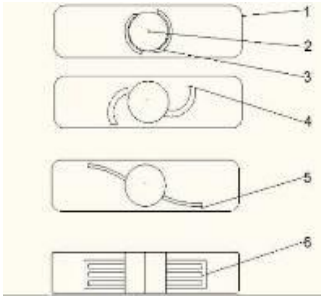

Fig.4. 3. Solution B – integrated wave breaker on the pump module;
1/top view; 2/module; 3/breaker in closed position; 4/top-breaker view during installation–opening phase; 5/breaker in position; 6/front view of the breaker - section

The solution highlighted in Fig. 4.3. is a wave breaker made of a malleable material with increased elasticity, which wraps itself on the delivery-pump module. After insertion into the tank, the wave breaker opens due to its elastic properties. As can also be seen in Fig. 4. 3., the length of the breaker may not cover the entire length of the model tank. The length is limited by the circumference of the delivery pump module. A simple solution is to design a wing with a length equal to half the circumference of the mode, but a wing of the length equal to the circumference of the module can also be achieved by a more complex design. By implementing the ski space in Fig. 4.3. the aim is to reduce the noise caused by the waves inside the tank breaking from its walls. In addition, in the case of a tank which had severed slosh noise performance without changing the envelop concept, this type of solution represents a potential for improvement at minimal cost.

4.2. Elaboration of 3D models for the anti-slosh noise Wing Baffler solution - embarked

Based on the arguments generated for the solution presented in Fig. 4.3, the development of 3D models was done to study in detail the possibility of implementing the designed solutions. For an overview, in Fig. 4.4 are highlighted: The Fuel Delivery module, Wing Wave breaker assembly, but also its integration within the generic tank [MAN15]. Following the deepening of this solution, it was found that:

Fig. 4. 4. Wave breakers integrated into the tank

- The presence of the float and its projections influences the length and shape of the wings;
- The possible movement of the module arm influences the areas of grip and insertion of the wings;
- The structure of the wings may present risks in terms of increased flexibility and open position in assembly operation;
- Number of limited wings;
- The length of the wings limited by the diameter of the Fuel Delivery module.

Fig. 4. 5. Closed-wing Module Ensemble

If the wings were finally folded around the module, now the wings are strapped together by overlapping. This type of folding does not interfere with the possible movement of the module arm and allows the length of the wing-type baffle to be stretched (Fig. 4. 5).

The assembly of the module equipped within the generic tank is shown in Fig.4.6. Introducing the module with the folded wings into the existing hole in the tank, intended to insert the Fuel Delivery module .

Fig. 4. 6. Tank assembly – closed wings - pre-assembly

In order to keep the wings in an open position and avoid the risk of over-extension, a technical solution has been adopted that involves the implementation of multiple ribs, at the base of the wings, and on the rest of the surface.

The equipped Fuel Delivery module comes with its wings in an open position. At the time of installation, the operator tightens/closes the wings on top of each other to facilitate the assembly of the module with the tank. The wings of the module have ribs for stiffening of the wings, so that during functioning keeps opened and perform their wave-breaking function [DEM12].

The general characteristics of the concept of Fuel Delivery module equipped with slosh noise baffle with wings inside a tank are:

- Insertion of the Wing Baffle in the same operation of insertion of the module into the tank;
- Use within an existing tank to improve the slosh noise benefit;
- Possibility to generate various shapes and sizes, depending on the design of the tank;
- Base for the study and development of other similar technical solutions.

Based on the design previously made for the solution presented in Fig. 4.4., keeping the main feature – the slosh noise baffle usable on existing tanks – a second concept was generated to solve the problems identified in the deepening of the concept «Wave breaker Type Wings» :

- The possible movement of the module floating arm influences the areas of grip /insertion of the wings;
- The structure of the wings may present risks in terms of increased flexibility and keeping the position open in operation;

- Number of limited wings;
- The length of the wings limited by the diameter of the pump mode.

4.3. Elaboration of 3D models for the "Link Baffle" slosh noise reduction solution

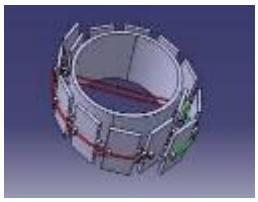

Fig. 4.7. Folded wing link type

To mitigate the risks of flexibility and wing position, it was considered to design a central support (Fig.4.7) that will be assembled on the Fuel Delivery module on which the baffle wings will be assembled in the fuel tank.

Making this support, changes one of the characteristics of the "Wing Baffle" concept, that of the insertion of the baffle at the same time with the Fuel Delivery module, but will solve the issues identified regards to the limiting the length of the wings, as well as their number. Previous design of the wings are modified so that they can be inserted with the central support before insertion of the Fuel Delivery module. For this, a new concept of wings, type "Link" (Fig. 4.7) was considered. The length of the wings can be given by the number of Links. This Links are connected to each other, directly with the help of pins, and a rigid cable will assure their interconnection. The number of Link type baffle wings may differ depending on the necessity and complexity of the project. The cable connects the Links with the central support, while also ensuring a connection of the wings, passing through the central body (Fig. 4.8–cable in free position). At the time of insertion of the pump Fuel Delivery module (Fig. 4.9), the cable will stretch and the tension of it will ensure a rigid and fixed position of the Links in functioning. The general characteristics of the Link slosh noise baffle solution concept are as follows:

Fig. 4.8. – Pre insertion MJP

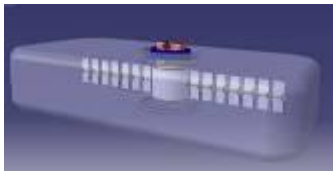

Fig. 4.9. – Final insertion of MJP

- The insertion of the baffle wings considered an easy solution for any technological manufacturing process.
- It can be used for an already existing tank design, which is intended to improve the slosh noise benefit.
- Possibility to generate various shapes and sizes, depending on the design of the tank.
- Base for the study and development of other similar technical solutions.
- Possibility of modifying the shapes of the central body, but also of the other elements, depending on the requirement.
- Possibility to add more interconnected structures.

Fig.4.9. Detail of adjacent flexible cylinder embarked on pump mode – fastening and positioning area / anti-rotation

Following a detailed analysis of the concept, it was found that some difficulties led to optimizations. As a result, an extensive process of optimizing the project has been carried out. Thus, the following solutions were implemented:

- Cutting the related cylinder (central support), both around the floating arm, and in the area of the vents (Fig. 4.9).
- The degrees of freedom were taken over by an anti-rot system between the connected cylinder and the Fuel Delivery module, as can be viewed in Fig. 4.9.
- The connection mode of the breaker has been redesigned to allow the assembly of a pin for locking on a larger surface. In addition to the pins, a guide and positioning channel was also developed. It also limits

the rotation between two Links. Larger areas require less precision in the manufacturing process, thus reducing the cost of execution for the Links.

- The spaces between the fairies have also been diminished to facilitate cable shortening. This measure improves the stability of the breaker after the assembly stage. For added efficiency, the area of passage of the cable through the za was modified by creating a contact area of a length like that of a tile, thus giving an added robustness to the assembly. The number of Links is defined according to the geometry of the tank in the.

Fig.4.10. Insertion of the baffle in the fuel tank

Fig.4.11. Baffle in pre-assembly stage

Fig. 4. 12. Central cylinder and interconnected cable-connected Links in not tensioned position, slightly flexible assembly

The idea of wrapping the structure of interconnected fairies around the module had to be partially abandoned. The attachment of the tiles to the additional cylinder has been preserved and the structure of interconnected cable tiles has a degree of flexibility due to the assembly tolerances allowing the breaker to be inserted into the tank with a positive impact on the assembly process carried out by the operator (Fig. 4. 10, Fig. 4. 11). The Links have a rectangular shape to allow the integration of the technical solution of self-locking and grip through the channel and pin. A circular Link solution does not favor complex assembly.

The cables pass on both sides of the Links (Fig. 4.12). They shall be straining when the Fuel Delivery module is progressively inserted. The length of the not tensioned cable is equal to the length of the tensioned cable. This ensures stiffness with the movements of the liquid in the tank.

According to the technical literature studied, the perforations in the baffle diminish the forces exerted by the waves over the assembly (Fig. 4.12) [HOI04].

4.4. Elaboration of 3D models for Fishbone Wave Breaker solution

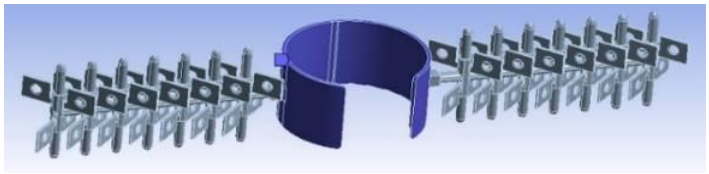

Fig. 4.13 – Fishbone slosh noise baffle

As in subchapters 4.3 and 4.4, the novelty is to create a technical solution for modular wave braking and adaptable to the geometry of an existing tank. The proposed solution is presented in Fig. 4.13 and is an adaptable baffle for several fuel tank typologies, using as a functional component complex module that forms the breaker's wing by assembling more such modules. Due to the shape of the resulting wing resembling a fish skeleton, the wave breaker was given the name "Fishbone".

The module that forms the wings is a complex component. Thus, the main constructive features are:

- The width of the rod is adjustable according to the width of the tank through the integrated spring (Fig. 4.14. Balloon 3) in the rod (Fig. 4.14, Balloon 2).
- To avoid aggression of the surface of the tank (upper/lower) use rubber finishes (Fig. 4. 14. Balloon 1).

- Flat surfaces represent the upper and lower wings that have the role of breaking the waves produced inside the tank. The gaps/cuts present in the geometry of the wings make the wave-breaking process more efficient.
- The length of the spring is adjusted according to the space available in the tank and its geometry. The assembly is done through the interconnection elements (Fig. 4.14, Balloon 5) in two stages:
- Position and partial introduction into the conjugated element (Fig. 4.15).
- Pushing the element into the conjugated element until triggering the self-locking system (Fig. 4.16). The assembly thus created is non-removable. In Fig. 4.17 observe an isometric view of subassembly.

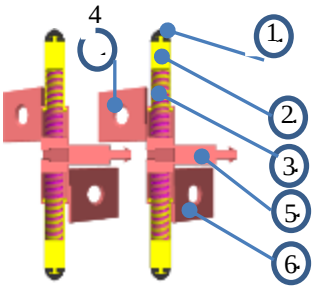

Fig. 4.14. Fishbone element
1. rubber plot / 2. Rod / 3. resort/ 4.upper wing/ 5. interconnection element/ 6. lower wing

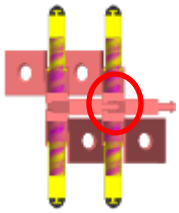

Fig. 4.15. Interconnection element – stage one

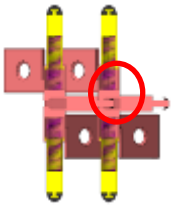

Fig. 4.16. Interconnected Element

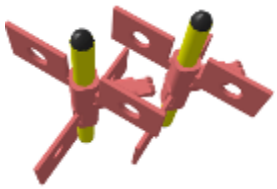

Fig. 4.17. Isometric View

Fig. 4.18. Cutting cylinder - Venturi area and Float

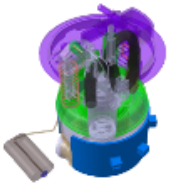

Fig. 4.19. Assemble cylinder on pump module

The interconnected elements are assembled on a cylinder connected to the Fuel Delivery module. The cylinder is cut with vents for the Fuel Delivery module Float (Fig. 4.18). It presents predefined areas to connect wave braking Fishbone modules. The areas will be used according to the geometry of the tank. The cylinder correlates with the position of the Fuel Delivery module and does not rotate. In Fig. 4.19 is presented the positioning and anti-rotation element model [FRA13]. The interconnected rods retain their assembly principle (Fig. 4.16) to be mounted on the cylinder (Fig. 4. 18).

CHAPTER 5: Static analysis of variants of slosh noise reduction systems developed

5.1. General considerations

The analysis aims to study the behavior of slosh noise baffle during working status. An analysis shall be considered based on the application of forces to the surfaces of the wave breaker in order to assess its resistance to breakage and its behavior to deformation.

Study the three slosh noise baffles models presented:
- „Wings" baffle solution.
- „Link" baffle solution.
- „Fishbone" baffle solution

The material considered for the analysis of the three types of slosh noise baffles is polypropylene - "a thermoplastic polymer, used in a wide range of applications: packaging, labelling, textiles, plastic parts, automotive components, etc. This thermoplastic polymer is very robust and incredibly resistant against many chemical solvents, acids and bases" [LUB15]. Some of its characteristics that we follow in this study are found in Table 5.1.

Tab. 5.1. Mechanical properties of polypropylene [ULP15]

Hardness, Rockwell R	20.0 – 118 HR
Traction resistance	9.00 - 80.0 MPa
Breaking resistance, yield	60 - 170 MPa
Breaking elongation	900 %
Bending resistance, yield	20.0 - 180 MPa
Compression resistance, yield	55.2 MPa

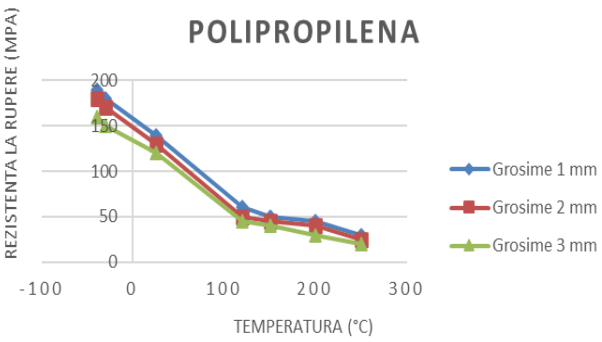

Fig. 5.1. Break resistance of polypropylene according to temperature [ULP15]

Note from Fig. 5.1. that the breaking resistance varies depending on the thickness of the material and the temperature of the environment in which it is used. Therefore, temperatures between -30 °C and 80 °C were considered at the level of the car fuel tank. Thus, we can consider the breaking resistance of polypropylene in the "Slosh Noise Baffle" application between 60-170 MPa (Fig. 5.1) [ULP15].

The calculation of the force applied by the study was carried out considering the maximum possible force with which the amount of liquid in the tank relative to the speed of travel (Tab.5.2).

Tab.5.2. Input parameters

Speed [km/h]	Time [s]	Speed [m/s]	Acceleration [m/s2]
10	1,39	2,78	2
30	3,65	8,33	2,28
50	5,40	13,89	2,57

Thus, according to the fuel volume and driving speed proposed in the study, the results presented in Tab. 5.3 were obtained.

Tab. 5.3. Calculation of forces applied according to addictive parameters

Fuel volume [L]	Diesel fuel Density [kg/L]	Mass [kg]	Force 10km/h [N]	Force 30km/h [N]	Force 50km/h [N]
15	0.832	12,5	25,1	28,6	32,2
25	0.832	20,9	41,8	47,6	53,6
35	0.832	29,2	58,5	66,6	75,1
45	0.832	37,6	75,2	85,7	96,6

The maximum force developed by the fuel fluid in the tank is 96.6 N for a diesel fuel volume of 45L, considering an acceleration from 0km/h to 50 km/h in 2.57 seconds.

So, for numerical simulations on deformation study performed using ANSYS V19.0 software, it will be considered a superior approximation of the maximum value of the force (96.6N) namely 100N.

5.2. Static analysis for The Wave Breaker Wings Type

5.2.1. Determination of study characteristics

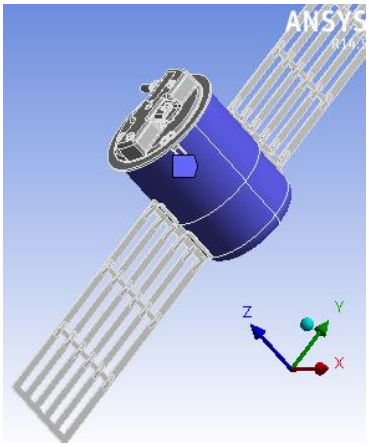

Fig. 5.2. Fuel delivery Module boarded with wing wave breaker

The fixed part of the assembly, the outer surfaces of the pump mode and the grip surfaces of the wings located on the module (Fig. 5.2) shall be considered as a fixed part of the assembly. At the same time, the vertical position of the module in the analysis system is considered.

5.2.2. Study of deformation

A force of 100 N perpendicular to the surface of the baffle wings shall be applied to determine its maximum theoretical deformation in the system.

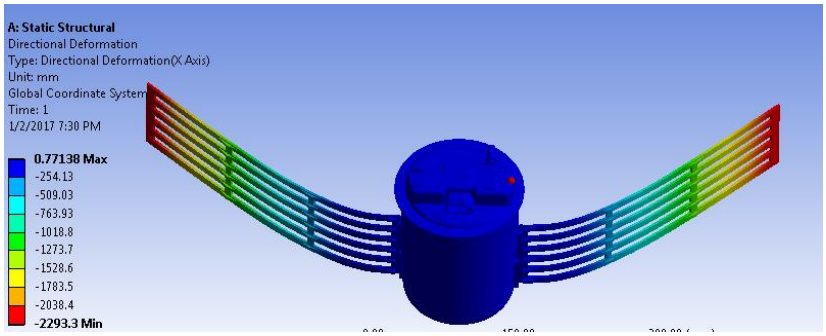

Fig. 5.3. Wing deformation – X Axis direction

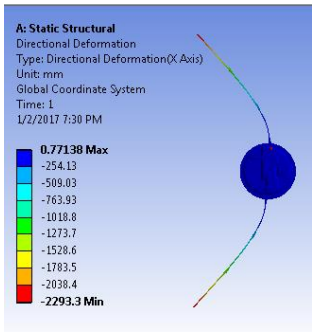

Fig. 5.4. Maximum wing deformation

A deformation of the wing can be observed in the direction of force application (Axis -X) of up to 2300mm (Fig. 5.3). Furthermore, deformation occurs along the length of the wing, and the degree of maximum deformation is present on the end of the wing and can reach 2300 mm from the original position. Behavior can be seen in plane XY in Fig. 5.4. This deformation value also concludes an elongation of the material in use.

5.2.3. Study on breaking resistance

For the purpose of studying breaking resistance, the same force of 100 N shall be applied to the surface of the wings. The Von Mises theory is applied to determine the risk areas. Specifically, if the baffle will withstand the required loading conditions. The concept of Von Mises stems from the theory of deformation energy. This is the comparison between two types of energies: the deformation energy in the current case and the deformation energy in a case of simple deformation at the time of breakage. According to this theory, rupture occurs when the deformation energy in real case is greater than the deformation energy in a case of simple voltage at the time of rupture [PHA16]. From the simulation (Fig.5.5) you can see the surfaces with the highest risk of breaking.

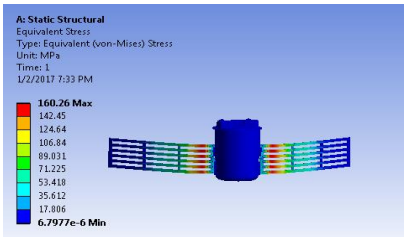

Fig. 5.5. Identification of breaking risk areas

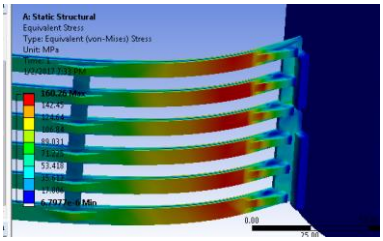

Fig. 5.6. Detail of the maximum risk zone at breakage

Considering the Von Mises theory, the baffle wing has the highest risk of breaking in the area indicated by the red color (Fig. 5.5) and in the grip area with the pump-beam module (Fig. 5.6), recording values of 160.26 MPa. Considering the material characteristics of polypropylene, i.e. the breaking resistance between 60 MPa and 170 MPa, under the given conditions, we can conclude that the material and the actual design/design pose a risk to breakage.

5.3. Static analysis for Link slosh noise baffle

The static analysis for the Link baffle was carried out using the same structure and input data as in the system in the previous study – Wave baffle Wings type. Depending on the scenario tested, for the study of extreme cases treated in numerical simulations, consideration will be given to:

- A force of 100N applied perpendicular to the surface of the baffle - the value of this force shall be considered the maximum possible upper rounded value in accordance with section 5.1 of this Chapter.
- A force of 30N applied to the lower part of the breaker, and its value represents 30% of the possible extreme value of a force, according to Tab. 5.3.
- A force of 20N applied to the last structure of the breaker, and its value represents 20% of the possible extreme value of a force, according to Tab. 5.3. and considers that the last Link within the baffle represents 20% of its structure.

5.3.1. Study on deformation

5.3.1.1. Deformation under the conditions of application of the force considered on the Link type slosh noise baffle assembly

A force of 100 N perpendicular to the wings of the Link Baffle shall be applied in the direction of the X-axis to determine theoretical deformation. Different behavior can be observed as opposed to of the previous case studied. In the case of the current analysis, a movement of the Links is observed following the application of force and a tension / deformation of the cable connecting them. The deformation of the material of the Links is almost non-existent. A total bending/deformation of the wings is obtained in the direction of the X-axis of up to 35 mm. (Fig. 5.7)

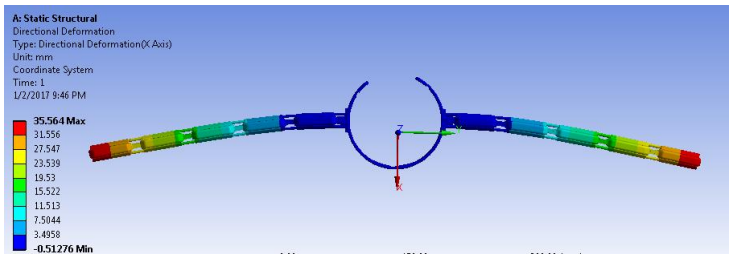

Fig. 5.7. Deformation areas at risk of breakage for the Link Baffle design

A force of 100 N perpendicular to the wings of the Link Baffle shall be applied in the direction of the X-axis to determine theoretical deformation. Different behavior can be observed as opposed to of the previous case studied. In the case of the current analysis, a movement of the Links is observed following the application of force and a tension / deformation of the cable connecting them. The deformation of the material of the Links is almost non-existent. A total bending/deformation of the wings is obtained in the direction of the X-axis of up to 35 mm. (Fig. 5.7)

5.3.1.2. Deformation when applying a force to the entire surface of a wing

A force of 100 N shall be applied to one the Baffle wings. Thus, a greater total wing deformation can be observed than in the previous case, i.e. 92 mm in the direction of force application (Axis X), (Fig. 5.8). The behavior of deformation is not linear on the surface of the wing, each Link of this breaker changing its position. Behavior can be observed in the XY plane according to Fig. 5.9. This deformation can be the displacement of the Links at the time of impact with the waves in the tank, which theoretically also respects the idea of this design in order to reduce the forces acting on the baffle.

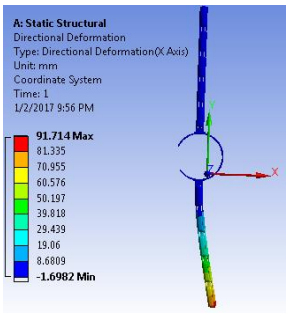

Fig. 5.8. Deformation of the Link Baffle

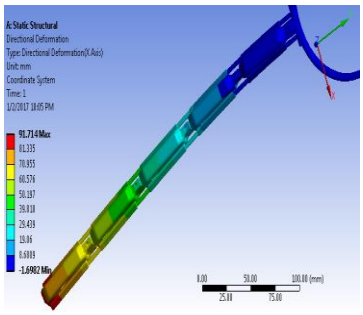

Fig. 5.9. Detail on structural deformation

5.3.1.3. Deformation of the Link subassembly following the application of a 20N force on the last Link of the baffle

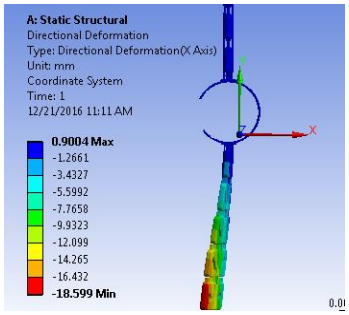

Fig. 5.10. The phenomenon of twisting the Baffle's wing following the application of a force of 20N on the last Link of the assembly

Due to this behavior it is necessary to apply independent forces on the Links of a wing in order to establish the conformity of this design. Thus, it is considered the application of a force of 20 N on the last Link of the Wing assembly, in the direction -X, considering a smaller amount of fuel that can act on the surface. An uneven deformation and a change in the shape of the entire surface of the baffle's wing can be observed in the XY plane. Thus, the upper wing area reaches a deformation of 18 mm on the X axis, and the lower area reaches a deformation of 9 mm on the X axis, practically producing a twist of the subassemblies, (Fig. 5.10). This shape change may lead to an increase in cable tension and its degradation.

5.3.1.4. Deformation when applying two forces to a wing

To conclude this, the application of an extreme force of 100 N on the upper area of the Links (Fig. 5.11) and a smaller force of 30N on the lower area is considered to highlight the deformability of the baffle.

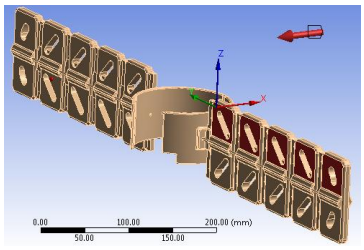

Fig. 5.11. Force application area

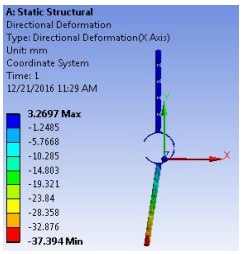

Fig. 5.12. Deformability of the assembly

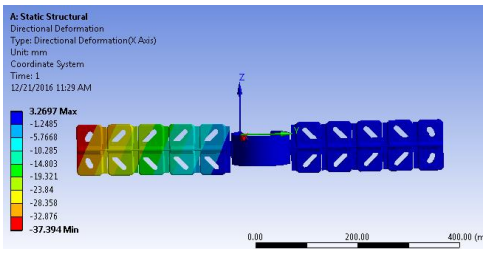

Fig. 5.13. Deformity of the ensemble – front view

The same behavior as the previous one can be observed, with a decrease in the difference in the level of deformation in the XY plane between the lower and upper part (Fig. 5.12). As with the application of an extreme force, which theoretically could not be achieved in operation, that only on an area of the baffle, the area deforms by a total of 37mm, without any deformation of the Link subassembly, the deformation being induced by the connecting cable (Fig. 5.13).

5.3.2. Study on breaking resistance

The breaking resistance of the assembly will be achieved by considering the application of the Von Misses theory on the three simulations applied in the case of the deformability study.

5.3.2.1. Break resistance under the force considered to be applied to the Link Baffle assembly

For the study, the simulation in 5.3.1.1., concerning the application of a force of 100 N on the Link Baffle assembly and using the Von Mises theory, shall be considered. Thus, an increase in tension can be observed in the connecting cable as well as in attachment of the Links on the maximum stretching area. (Fig. 5.14, Fig.5.15)

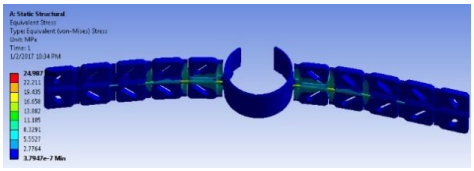

Fig. 5.14. Highlighting the Tension in the connecting cable

Fig. 5.15. Highlighting the risk area for breaking the connecting cable

In detail (Fig. 5.16, Fig. 5.17), there is an increase in tension in the connecting cable material of up to 25 MPa and in the Link material, in the grip area, up to 22 MPa. Considering as a material for Link polypropylene, the baffle will withstand exposure to a force of 100 N, polypropylene having the resistance to breakage between 60-170 MPa. In the case of a steel connecting cable, it will withstand breaking under these conditions due to its breaking resistance between 1500-2500 MPa [ULP15].

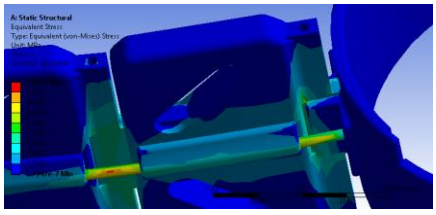

Fig. 5.16. Detail of the area in risk of breaking – front view

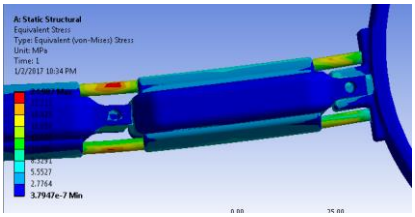

Fig. 5.17. Area with risk of breakage – top view

5.3.2.2. Break resistance when applying force to the entire surface of a wing

In this case, following the application of a force of 100 N on the surface of a wing, it can be observed the increase of the probability of breakage only in the catchment area of the Links with fixed support, (Fig. 5.18). In detail (Fig. 5.19, Fig. 5.20), two areas where deformation can lead to breakage are observed. One of the areas is the area of the end-key, where friction with the fixed support may occur due to the deformation of the assembly. In this area the material reaches a maximum voltage of 30-35 MPa, which means that the material will withstand breakage when using polypropylene, this having the resistance to breakage between 60-170 MPa.

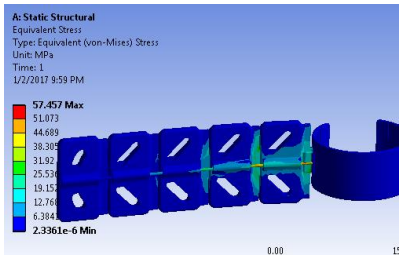

Fig. 5.18. Deformability of the assembly

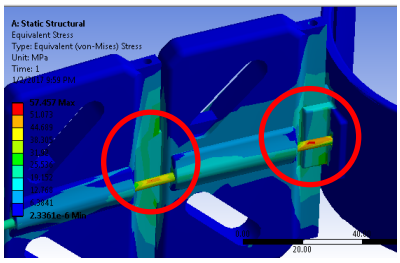

Fig. 5.19. Detail on cable breaking resistance - side view

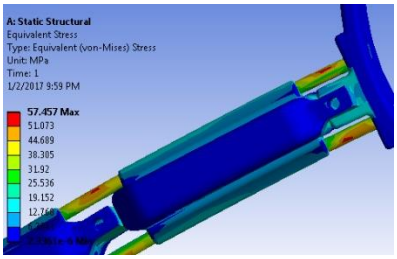

Fig. 5.20. Cable breaking resistance detail – top view

An increase of tension up to 60 MPa can be noticed in the fixing cable.

5.3.2.3. Breaking resistance when applying a force on one subassembly

In this simulation, it is considered the application of a force of 20 N on the last Link of the wing (Fig. 5.21, Fig. 5.22). If in the case of deformation, a displacement of the wing in two planes has been observed, in the case of breaking resistance, the forces acting in the material do not exceed 15 MPa. Considering the 60-170MPa limit of breaking resistance in the case of polypropylene, in this case, the Baffle will resist.

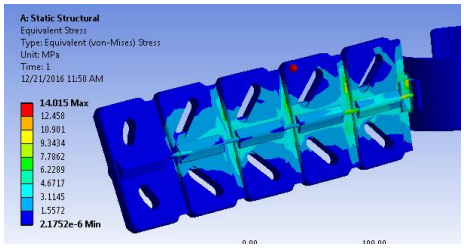

Fig. 5.21. Deformability of the assembly

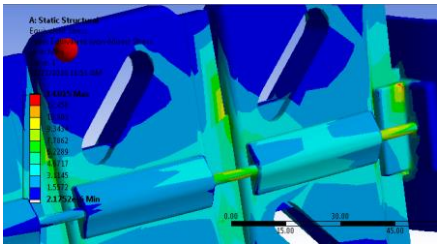

Fig. 5.22. Risk area detail

5.3.2.4. Break resistance when applying extreme force

The third simulation confirms the results of the first simulation. Thus, in the case of the application of extreme forces in the upper area of the Links, forces can be observed on the surface of up to 82 MPa on the area of the fixing surface of the Links (Fig. 5.23, Fig. 5.24).

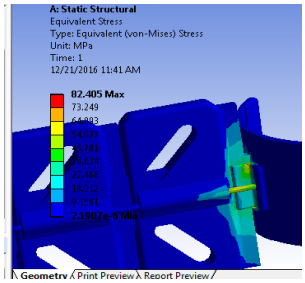

Fig. 5.23. Highlighting the risk zone

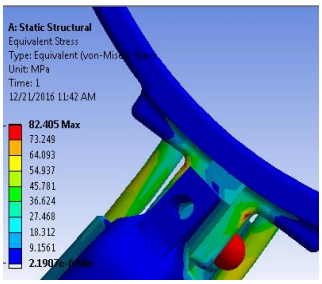

Fig. 5.24. Risk area detail

Therefore, under normal conditions of use, the wave breaker will withstand breakage and can change its shape/position by up to 35 mm. This concept has a much safer design than the Wing Baffle solution.

5.4. Static analysis for Fishbone slosh noise baffle

Static analysis for the Fishbone Baffle (Fig.5.25) was performed using the same structure and the same system input data as for the study of the Link Baffle.

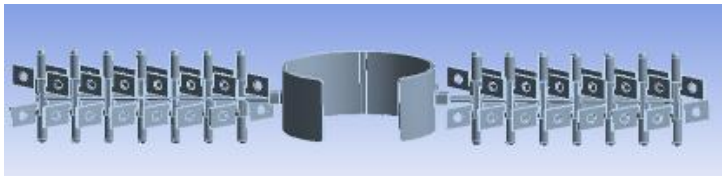

Fig. 5.25. Fishbone Baffle

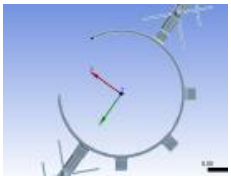

Fig. 5.26. Fixing cylinder detail

5.4.1. Study on deformation

5.4.1.1. Deformation in case of application of force on the wing

In order to determine the degree of deformation, a force of 100 N can be applied to one of the wings in the direction of the X-axis. Thus, deformation occurs between 0.3 mm and 1.8 mm (Fig. 5.27). In addition, a slight twisting of the blades can be observed (Fig. 5.28).

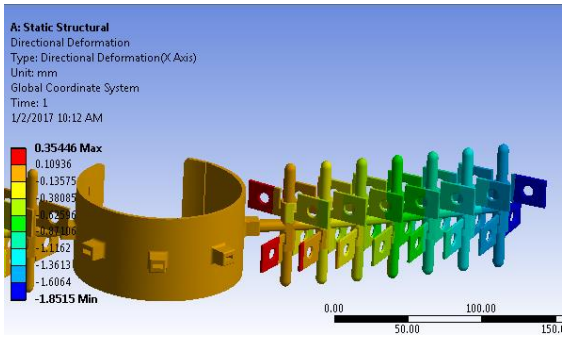

Fig. 5.27. Deformability of the Fishbone assembly

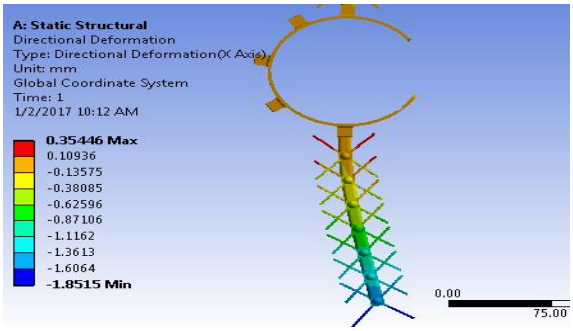

Fig. 5.28. Top view of the deformability of the assembly

5.4.1.2. Deformation when applying a force to the pallet subassembly

Due to this behavior, independent forces are needed to be applied to the blades of a wing in order to determine their efficiency and strength, (Fig. 5.29).

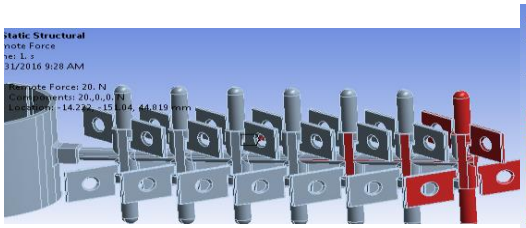

Fig. 5.29. Strengths applied independently on the blades of a wing

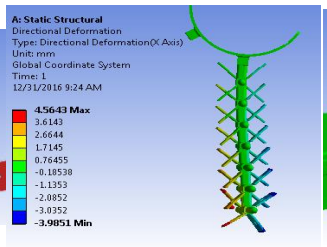

Fig. 5.30. Breaker deformability

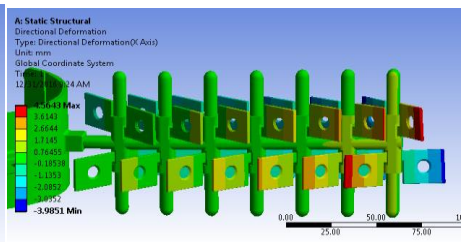

Fig. 5.31. Deformability Detail

Thus, it is considered to apply a force of 20 N on the last set of pallets, in direction X, considering a smaller amount of fuel that can act on the surface. Uneven deformation and a change in the shape of the blades and the wing can be observed in the XY plane (Fig. 5.30, Fig. 5.31).

Thus, the deformation of the wing reaches 4 mm on the X axis including a deformation of some pallets.

5.4.1.3. Deformation in the case of the application of extreme forces

In order to check the deformability of the assembly, an extreme force will be applied as in the case of the Link Baffle. A force of 100 N shall be applied to the upper part of the wing structure and a force of 30N to the lower area to highlight the deformability of the assembly. The increase in deformation in the XY plane can be observed to 7mm in the direction of the X axis, the smallest deformation of the three types of breakers studied (Fig. 5.32, Fig. 5.33).

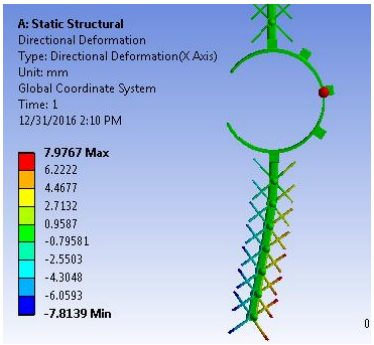

Fig. 5.32. Ensemble deformation – top view

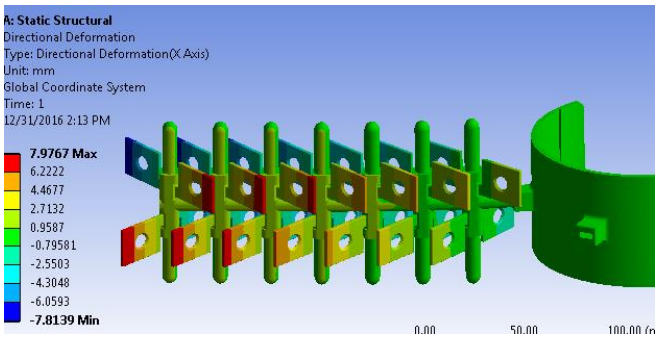

Fig. 5.33. Ensemble deformation – front view

5.4.2. Study on breaking resistance

The three cases of simulations shall be considered in order to study and highlight the breaking resistance of the Fishbone type assembly and its pallets.

5.4.2.1. Break resistance when applying a uniform force to the wing surface

A force of 100 N shall be applied to the direction of the X-axis to the surface of a wing of the Baffle. It can be seen in figure 5.34 the appearance of tension in the material only in the areas of attachment of the blades.

Thus, the greatest risk of breaking in the catchment area of the Fishbone assembly with the fixed central area (Fig. 5.35) is recorded. Considering the breaking resistance between 60-170 MPa it can be considered that the assembly resists breaking in operation.

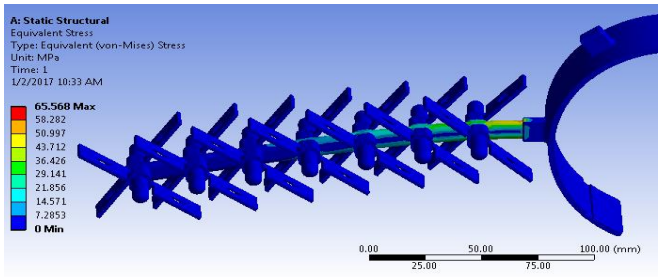

Fig. 5.34. Tension area – overview

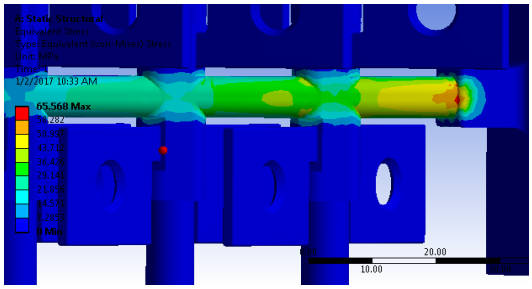

Fig. 5.35. Maximum tension area detail

An accumulation of tension in the material can be seen in the catchment area with the fixed assembly of the Fishbone type breaker. The effect is similar in all three baffles analyzed.

5.4.2.2. Break resistance when applying a force to pallet subassembly

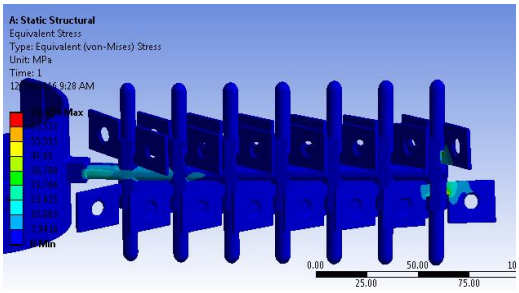

Fig. 5.36. Breaking risk areas – overview

Following the application of a force of 20 N on the pallet subassembly located at the free end of a wing, material tension accumulations (Fig. 5.36) can be observed both on the wing arm (15-30 MPa) and at the pallet level in the contact area with the arms of the subassembly (15-70 MPa).

Considering the properties of the material, it can be concluded that the resistance of the assembly to breakage is greater than the simulated values.

5.4.2.3. Break resistance when applying extreme forces

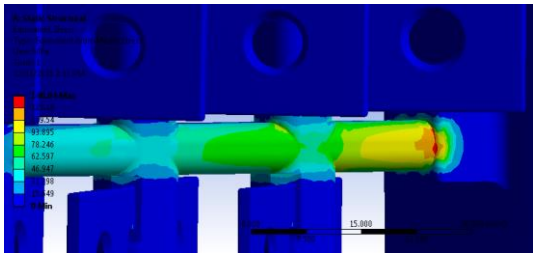

Fig. 5.37. Detail of breaking area

Following the application of 100 N forces to the upper area of the assembly and an additional force of 30 N to the lower area, increased tension in the material in the wing grip area with the fixed support is observed. This confirms the initial study. The material may fail (Fig. 5.37) in case of use under high temperatures (>50°C), polypropylene may enter the plastic deformation zone.

Considering the results of this static analysis, the Fishbone wave breaker has less deformations than the previous concepts studied, but may pose a breaking risk when applying forces leading to the twisting of the wing subassembly.

5.5. Conclusions and research directions

Following the static analysis of the three models, in the case of normal use, the following are concluded:

1. The Wing slosh noise reduction Baffle has a wing deformation of 2300mm and a risk of breaking the wings, the largest deformation of the three concepts analyzed.
2. The Wing slosh noise reduction Baffle presents a risk of breakage, the material being able to yield at 180 MPa, considering the application of a force of 100 N perpendicular to the wings. This concept will be abandoned for future studies.
3. The Wing slosh noise reduction Baffle has the greatest deformation of the wing under normal operating conditions >13mm. Thus, it will not proceed to the stage of making prototypes to confirm results by carrying out physical tests.
4. Under normal conditions of use, the Link slosh noise reduction Baffle will withstand breakage and can change its shape/position by up to 35mm.
5. The Fishbone slosh noise reduction Baffle shows the slightest deformation of the wing under normal operating conditions <5mm.
6. For use in extreme conditions it is recommended to use a material with polypropylene-like properties but with a breaking resistance >100 MPa.
7. For Link and Fishbone slosh noise reduction baffles, the analysis will continue to demonstrate efficiency on the modeling of dynamic fuel behavior in the vehicle tank.

CHAPTER 6: Dynamic analysis by mathematical modeling of the movement of fuel waves in a tank, with and without slosh noise baffles

6.1. Introduction

The slosh noise phenomenon, which occurs in a tank filled with liquid, when braking, after its movement at a uniform speed, has been studied by various methods: analytical, numerical or experimental. [LAZ00] [IAC52]

The analytical method involves the use of the potential formulation to define the free surface of the fuel, which is an (almost) incompressible fluid. In some cases, the theory of potential is not sufficient, the determination of the free surface inside the tank being closely related to the correct approximation of the sound generated by the liquid wave, but can be used as a useful first approximation in later modeling.
The numerical method involves different approaches in the analysis of the slosh noise phenomenon that occurs in a closed fuel tank, of which one can list: (1) approximation of MAC (Marker and Cell), (2) approximation of the volume of fluid VOF (Volume of Fluid Method), Method LSM (Level Set Method) or (3) a combination of these methods. More recently, the Approximation of SPH (Smoothed Particle Hydrodynamics) (4) was used in 2D numerical approximations to simulate sound propagation [SAG18].

Regardless of the approach, the main variables on which the slosh noise phenomenon depends are:

- the depth of the liquid;
- the geometry of the tank;
- frequency and amplitude of the initial external force acting on the tank.

To reduce this acoustic phenomenon, various types of slosh noise baffles can be installed in the tank. Their role is to reduce both the pressure on the ceiling or walls, as well as the phenomena manifested in the liquid, including that of slosh noise.

Any mathematical modeling involves identifying the legacies that come into the process by describing the sizes and links between them.

6.2. Description of the problem

In order to model mathematically the slosh noise phenomenon that manifests itself in a tank mounted on a vehicle that brakes suddenly, after being in motion at uniform rectilinear speed, the general assumptions related to the movement of fluid (fuel) will be specified for a start.

Modeling is a method of knowledge that consists of replacing the actual process with a model whose result is accessible and interpretable. The model is a simplified representation of the real process by describing the overall behavior of the essential forces involved in the process.

Assimilate the liquid in the tank to the vehicle tank with a material system $\mathcal{M}$ in relation to which working assumptions, sizes and symbols will be used, as set out below.

A. Assumptions

1. The mass is an additive measure;
2. The mass of the system remains constant in relation to time;
3. The kinetic moment of an elementary unit is given by the relationship[2]: $\int_D \rho \vec{x} \times \vec{v} dv$.

2The elemental unit, in the context of this modeling, is a point volume of liquid that behaves uniformly and retains the general characteristics of the liquid to which it belongs

B. Measures/symbolizations

„P" is a part of the system (tank);

"m" means the mass of the system, (m>0);

“D” is the volume occupied by the Part P (e.g. the volume part of the fluid volume in the tank);

$\vec{x}$ represents the position vector of an elementary unit of fluid-punctiform dimension;

¨ρ¨ represents the density of the fluid, measured at the level of an elementary unit as a function of time and position of that unit.

The slosh noise phenomenon is based on principles of continuous movement of environments, governed by different constituent laws, and follows the thermodynamic principles, all detailed in the following.

6.3. Formulating Mathematical Models

The phenomenon of slosh noise in a tank on a vehicle that brakes suddenly after being in motion at a uniform rectilinear speed is studied. General assumptions about fluid movement will be specified. The two modelling, analytical (MA) and numeric (MN) will be presented in parallel.

6.3.1. Analytical model (MA) for a tank without a slosh noise reduction baffle

Assumptions:

- The effects of liquid compressibility, viscosity and surface tension are neglected.
- The movement is irrotational.
- It is also assumed that the movement of the fluid is laminar in the z direction, so the movement is flat. [SU016]

The following notations are made:

1. L = tank width [mm],
2. b = tank length [mm],
3. ν= molecular viscosity,[Pa s] or [kg m^{-1} s^{-1}]

From the mass conservation equation, we can write:

$$\mathrm{div}\vec{v} = 0, \quad (1)$$

Noting $\phi = \phi(x,y,t)$ potential for speed, we have:

$$\vec{v} = \nabla\phi \text{ or } u = \frac{\partial\phi}{\partial x},\ v = \frac{\partial\phi}{\partial y}, \quad (2)$$

$$\Delta\phi = 0 \quad (3)$$

where :

- The speed vector $\vec{v}$;
- ¨$u = \frac{\partial\phi}{\partial x}$¨ and ¨$v = \frac{\partial\phi}{\partial y}$¨ represents the decomposed velocity vector in directions X and y respectively;

6.3.1.1. Initial state of the tank without a slosh noise reduction baffle, fig.6.1:

Boundary conditions: $\frac{d\phi}{dn} = \vec{v}\cdot\vec{n}$ are specified as follows:

On the side walls: $\frac{\partial\phi}{\partial x}(-l,y,t) = \frac{\partial\phi}{\partial x}(l,y,t) = 0$ (4)

On the floor: $\frac{\partial\phi}{\partial y}(x,0,t) = 0$ (5)

Conditions on the free surface: $y = \eta(x,t)$

Cinematic condition: $$\frac{\partial \eta}{\partial t} - \vec{v} \cdot \nabla \eta - \frac{\partial \phi}{\partial y} + \frac{\partial \eta}{\partial x} \cdot \frac{\partial \phi}{\partial x} = 0 \quad (6)$$

Dynamic condition: $$\frac{\partial \phi}{\partial t} - \vec{v} \cdot \nabla \phi + \frac{1}{2}(\nabla \phi)^2 + g\eta = 0 \quad (7)$$

where: ¨g¨ represents gravitational acceleration;
¨ϕ¨ potential of speed, ¨η¨ represents the amplitude of the free surface;

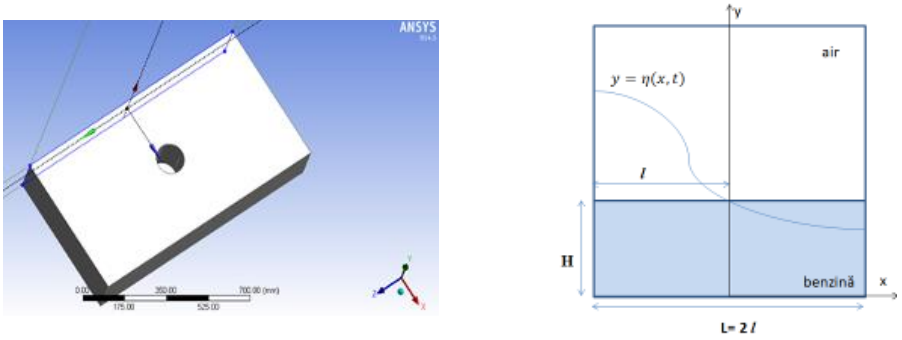

a) Geometry of the non-stop tank used in ANSYS for (LCY) b) Geometry of non-stop tank used for (MA)

Fig. 6.1. Tank geometry

Figure 6.1.a shows the coordinate system associated with the tank so, in direction x is considered the width of the tank (520mm), in the direction Z is considered the length (1000mm), and in the direction Y is considered the height of the tank (160mm). Origin is considered on the floor, in the center.

Figure 6.1b notes with H the height of the liquid in the tank.

As the liquid is incompressible, the potential energy of a liquid element is given only by the potential gravitational energy [ANS13] [CHU18] [DEM18]:

$$U^e = \frac{1}{2}\rho g b \int_0^a \eta^2(x,t)\, dx \ , \quad (8)$$

The kinetic energy of the liquid element is given by [CHU18] [DEM18]:

$$T^e = \frac{1}{2}\rho \int_V (\nabla \phi)^2 \, dV \quad (9)$$

where:
- ¨U^e represents the potential energy;
- ¨T^e ¨represents kinetic energy.

When the tank is subjected to a horizontal acceleration, $\ddot{X}_0(t)$, lateral sounds of the contained fluid will appear, where:

$$\dot{X}_0(t) = \begin{cases} U_0 - at, t \in [0, t_1] \\ -at_1, t \in [t_1, t_s] \end{cases} \quad (10)$$

where:
t_s is the total stop time of the tank ($t_s = 5s$) , $t_1 = 0.4s$, $a = U_0/t_1$.
¨a¨ represents the average value of the acceleration (braking in our case)

Movement in the tank is described by the potential ϕ, which breaks down into two functions.

$$\phi = \varphi + \psi \quad (11)$$

- φ solution of Laplace's equation with static conditions on the walls:

$$\varphi = xu + yv \quad (12)$$

ψ satisfies Laplace's equation: $\Delta\psi = 0$ in D (13)

and

on the side walls: $$\frac{\partial\psi}{\partial x}\left(-\frac{L}{2},y,t\right)=0=\frac{\partial\psi}{\partial x}\left(\frac{L}{2},y,t\right), \quad (14)$$

on the floor of the tank: $$\frac{\partial\psi}{\partial y}=0|_{y=0} \quad (15)$$

on the free surface: $$\mathrm{y}=\eta(x,t),\mathrm{H}=\eta(x,0)$$

$$\frac{\partial\eta}{\partial t}-\frac{\partial\psi}{\partial y}+\frac{\partial\eta}{\partial x}\cdot\frac{\partial\psi}{\partial x}=0, \quad (16)$$

$$\frac{\partial\psi}{\partial t}+\mathrm{y}\dot{u}+\mathrm{x}\dot{v}+g\eta+\frac{1}{2}\left(\frac{\partial^2\psi}{\partial x^2}+\frac{\partial^2\psi}{\partial y^2}\right)=0, \quad (17)$$

6.3.1.2. Analytical model (MA) for determining speed potential. Linear theory

The potential will be determined using the superposition method of the liquid's own functions in the tank, based on the linearized theory of potentials, compared to the nonlinear Boussinesq model [SU016].

Speed potential verifies the equations: $\Delta\phi=0$, on wet surface $\nabla\phi\cdot\vec{\mathrm{n}}=0$ (18)

We use the method of fundamental solutions, also described in [SU016], [LIN19] and consider that the potential has the

$$\psi(x,y,t)=\psi_0(x,y,t)+\sum_n\psi_n(x,y,t) \quad (19)$$

where

$$\psi_n(x,y,t)=\mathrm{f}_n(x,y)A_n(t) \quad (20)$$

are fundamental solutions that verify the Laplace equation with the conditions (13)-(16).

$$\Delta\mathrm{f}_n=0,$$
$$\frac{\partial\mathrm{f}_n}{\partial x}\left(-\frac{L}{2},y\right)=0=\frac{\partial\mathrm{f}_n}{\partial x}\left(\frac{L}{2},y\right),\frac{\partial\mathrm{f}_n}{\partial y}=0|_{y=0} \quad (21)$$

and linear conditions on the boundary:

$$\frac{\partial\eta}{\partial t}-\frac{\partial\psi}{\partial y}=0,\frac{\partial\psi}{\partial t}+g\eta=0, \quad (22)$$

and potential $\psi_0(x,y,t)$ is a particular solution that takes into account the movement of the tank, checks Laplace's equation and non-homogeneous conditions on the boundary:

$$\Delta\psi_0=0,\frac{\partial\psi_0}{\partial x}\left(-\frac{L}{2},y,t\right)=\dot{X}(t)=\frac{\partial\psi_0}{\partial x}\left(\frac{L}{2},y,t\right),\frac{\partial\psi_0}{\partial y}=0|_{y=0} \quad (23)$$

on the free boundary:

$$\frac{\partial\eta_0}{\partial t}-\frac{\partial\psi_0}{\partial y}=0,\frac{\partial\psi_0}{\partial t}+g\eta_0+\varepsilon\psi_0=0,\mathrm{y}=\eta_0(x,t) \quad (24)$$

For $n\geq 1$, $\varepsilon=0$ (in linear theory) we get $\frac{\partial^2\psi_0}{\partial t^2}=-g\frac{\partial\eta}{\partial t}=\frac{\partial\psi_0}{\partial y}$. (25)

Thus $\mathrm{f}_n(x,y)$ and $A_n(t)$ separating variables: $-\frac{\ddot{A}_n(t)}{A_n(t)}=\frac{g\frac{\partial f}{\partial y}}{\mathrm{f}_n(x,y)}=\omega_n^2$ (26)

we find the equations $\mathrm{gf}_{n,y} - \omega^2 \mathrm{f}_n = 0, \ddot{A}_n(t) + \omega_n^2 A_n(t) = 0$ (27)

The potential has the form $\psi_n(\mathrm{x},\mathrm{y},\mathrm{t}) = \mathrm{f}_n(\mathrm{x},\mathrm{y})\sin(\omega_n \mathrm{t})$, ω_n – angular frequency. (28)

For this case, the fundamental functions are:

$$\mathrm{f}_n(x,y) = -K_n \cos\big(\lambda_n(x+l)\big)\, ch(\lambda_n y) \quad (29)$$

$$A_n(t) = \sin(\omega_n t) \quad (30)$$

Where ω_n are the natural frequencies: $\omega_n^2 = g\lambda_n \,\mathrm{th}(\lambda_n H)$, $\lambda_n = n\pi/L$,checking on the free boundary the conditions:

$$\frac{\partial \eta_n}{\partial t} - \frac{\partial \psi_n}{\partial y}(x, \eta_n(x,t)) = 0, \frac{\partial \psi_n}{\partial t}(x, \eta_n(x,t)) + g\eta_n = 0, \quad (31)$$

$\eta_n(-l,0) = H$ leads to the determination of constants $K_n = \dfrac{gH}{\omega_n ch(\lambda_n H)}$ (32)

$$\eta_n(x,t) = \frac{\omega_n K_n}{g}\cos\big(\lambda_n(x+l)\big)\, ch(\lambda_n H)\cos(\omega_n t) \quad (33)$$

The amplitude of the free surface is:

$$\eta(x,t) = \eta_0(x,t) + \textstyle\sum_n \eta_n(x,t), \quad (34)$$

To determine the potential $\psi_0(x,y,t)$ and amplitude $\eta_0(x,t)$ solve the problem (21)-(22), where $\dot{X}(t) = U_0 - at, a \neq 0$ corresponding to braking.

$$\psi_0 = A_0(t) + (U_0 - at)x, \eta_0(l,0) = H, \eta_0(x,t) = -\frac{1}{g}\frac{\partial \psi_0}{\partial t}. \quad (35)$$

To determine the amplitude $A_0(t)$ pendulum equation is used [SU016]:

$$\ddot{A}_0 + B_1\dot{A}_0 + \omega_1^2 A_0 = \ddot{X}, B_1 = \frac{\sqrt{2\omega_1 \nu}}{Lb}\left(b + L + b\frac{\lambda_1(L-2H)}{\mathrm{sh}(2\lambda_1 H)}\right). \quad (36)$$

Under the given problem:

$$\Delta = B_1^2 - 4\omega_1^2 > 0, \quad (37)$$

Noting $\delta = \sqrt{\Delta}$ and $r_{1,2} = \frac{-B_1 \pm \delta}{2}$ $s$the solution of the equation has the form:

$$A_0(t) = \begin{cases} A_{01}, t \in [0, t_1] \\ A_{02}, t \in [t_1, t_s] \end{cases} \quad (38)$$

$$A_{01}(t) = c_{11}e^{r_1 t} + c_{12}e^{r_2 t} - \frac{a}{\omega_1^2},\ t \in [0, t_1], \quad (39)$$

$$A_{02}(t) = c_{21}e^{r_1 t} + c_{22}e^{r_2 t}, t \in [t_1, t_s]. \quad (40)$$

Constants c_{11}, c_{12} , c_{21}, c_{22} will be determined from the initial conditions as:

$$c_{11} = \frac{\dot{A}_0^1(0) - (A_0(0) + \frac{a}{\omega_1^2})r_2}{\delta}, c_{12} = \frac{(A_0^1(0) + \frac{a}{\omega_1^2})r_1 - \dot{A}_0^1(0)}{\delta},\ r_1 - r_2 = \delta\,. \quad (41)$$

$$c_{21} = \frac{\dot{A}_0^2(0) - A_0^2(0) r_2}{\delta}, c_{22} = \frac{A_0^2(0) r_1 - \dot{A}_0^2(0)}{\delta}. \quad (42)$$

For the given issue we consider conditions compatible with relationships (92) and (100):

$$A_{01}(0) = 0,\ \dot{A}_{01}(0) = al - gH,\ A_{02}(0) = A_{01}(t_1),\ \dot{A}_{02}(0) = \dot{A}_{01}(t_1), \quad (43/113)$$

Thus:

$$A_{01}(t_1) = c_{11} e^{r_1 t_1} + c_{12} e^{r_2 t_1} - \frac{a}{\omega_1^2},\quad \dot{A}_{01}(t_1) = c_{11} r_1 e^{r_1 t_1} + c_{12} r_2 e^{r_2 t_1} \quad (44/114)$$

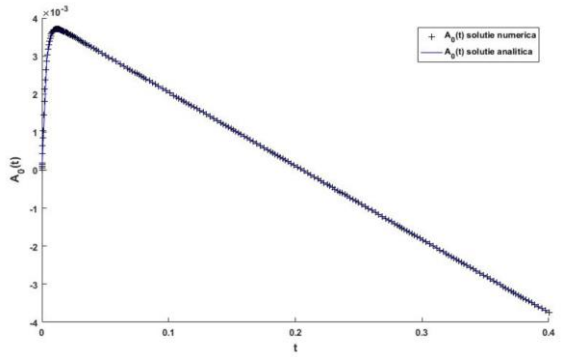

Fig. 6.2a. Evolution of zero amplitude by time, $t \in [0, t_1]$, t=0.4s, according to relationships (38), (43), (44)

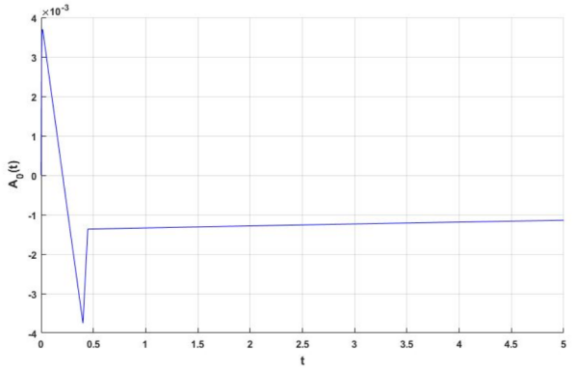

Fig. 6.2b. Evolution of zero amplitude (A_0 [m]) depending on time, $t \in [0, t_s]$, t=5s, according to relationships (38), (43), (44)

To make the graph in Figure 6.2a, an own computing code was created in MatlabR2016.R .

Thus, in the case of a tank without a breaker, it is observed that the braking time determines the maximum amplitude. It then drops to 0.4s (fig. 6.2a), following a slight climb and stagnation, which is the "quietness" of the waves inside the tank.fig. 6.2b).

In a fuel tank that does not have technical solutions for breaking waves, a large wave is observed followed by successive smaller waves that will hit each other (fig. 6.3a and fig. 6.3b). Thus, the noise generated represents the phenomenon of slosh noise, unpleasant for the user.

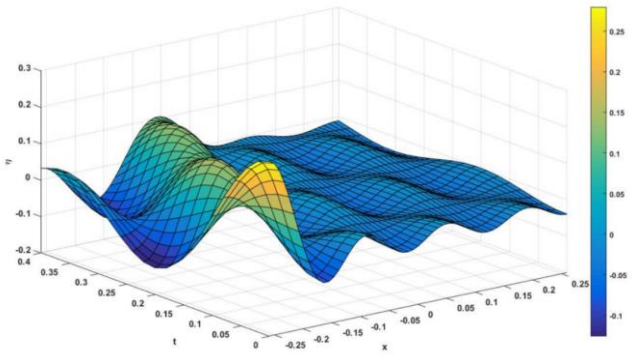

Fig. 6.3a. Evolution of the free surface for $t \in [0, t_1]$, t=0,4s, according to relationships (33) și (34)

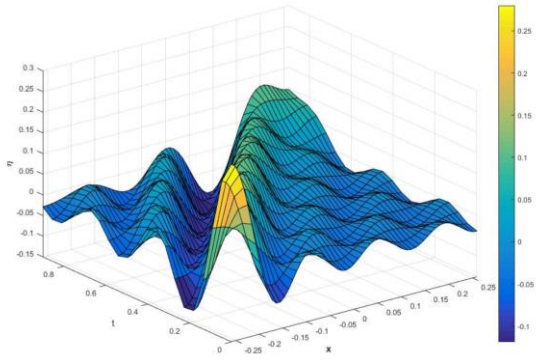

Fig. 6.3b. Evolution of the free surface for $t \in [0, t_1]$, t=0,8s, according to relationships (33) și (34)

To make the graphs in figures 6.2b, 6.3a and 6.3b, an own computing code was created in Matlab R2016.R, as detailed in the thesis.

6.3.1.3. Boussinesq's non-linear model with a slight disturbance of amplitude

The linear conditions on the free surface will change [SU016]

Cinematic: $\frac{\partial \psi}{\partial t} + g\eta + \varepsilon\psi = 0$ (45)

Dynamic: $\frac{\partial \eta}{\partial t} - \frac{\partial \psi}{\partial y} = 0$ (46)

From which removing the variable η we get: $\psi_{tt} + \varepsilon\psi_t + g\psi_y = 0$ (47)

6.3.2. Analytical model (MA) for a wave breaker tank [CHU18], [LU015]

Initial status of wave breaker tank, fig.6.4.:

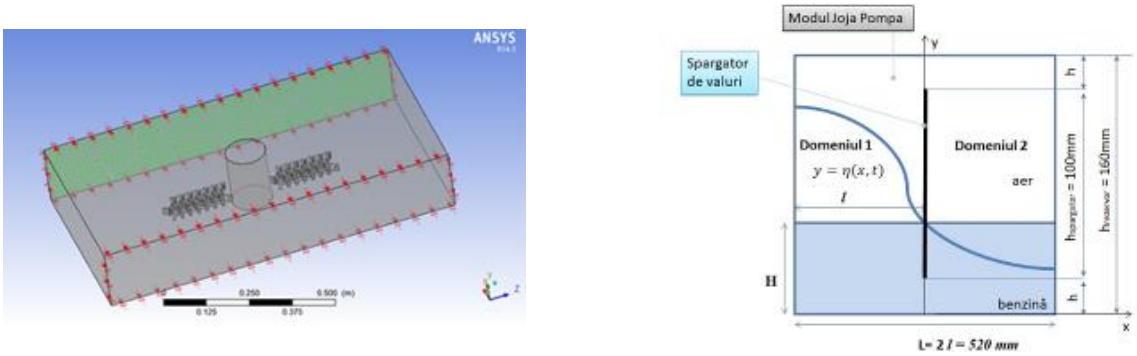

a) The geometry of the Baffle tank used in ANSYS for (MN)

b) The geometry of the Baffle tank used for (MA)

Fig.6.4. Geometry of tank with slosh noise baffle integrated

We consider the movement of the free surface on the width of the tank, flat movement, in the transverse plane and being the same along the length of the tank.
where:

h = 30mm,
Length of tank = 1000mm,
Tank width (L)= 520mm,
Tank height = 160mm

According to the geometry shown in Figure 6.4.b, movement in the tank is broken down into two areas. Potential $\phi = \varphi + \psi$ verifies Laplace's equation (13) with the shape (19), and ψ (13) in both areas $D_1 \cup D_2 = D, D_1 = [h, h + h_{sp}] \times [-l, 0]$,
$D_2 = [h, h + h_{sp}] \times [0, l]$, with notation $h_{sp} = h_{spărgător}$:

- it's his side walls D_1:
$$\frac{\partial \psi}{\partial x}\left(-\frac{L}{2}, y, t\right) = \dot{X}(t), \frac{\partial \psi}{\partial x}(0_-, y, t) = f(t), y \in [h, h + h_{spargator}] \quad (48)$$
- on the side walls of D_2:
$$\frac{\partial \psi}{\partial x}(0_+, y, t) = 0, \frac{\partial \psi}{\partial x}\left(\frac{L}{2}, y, t\right) = \dot{X}(t), y \in [h, h + h_{sp}] \quad (49)$$

- on the floor of the tank

$$\frac{\partial \psi}{\partial y} = 0|_{y=0} \quad (50)$$

- jump condition on the two sides of the breaker

$$\left[\frac{\partial \psi}{\partial t}(x,y,t)\right]\Big|_{-}^{+} = \frac{\alpha}{2}\frac{\partial \psi}{\partial x}\left|\frac{\partial \psi}{\partial x}\right| + 2C\frac{\partial^2 \psi}{\partial x \partial t}. \quad (51)$$

- condition of speed continuity at the level of $y = h$, pass from the liquid field without baffle, at level $y > h$, where the liquid is separated from the breaker in the fields D_1 and D_2:

$$\frac{\partial \psi}{\partial x} = u_{fsp}(x,t)\Big|_{y=h}, x \in [-l, 0] \text{ for determining the solution in } D_1 \quad (52)$$

$$\frac{\partial \psi}{\partial x} = u_{fsp}(x,t)\Big|_{y=h}, x \in [0, l] \text{ for determining the solution in } D_2 \quad (53)$$

$u_{fsp}(x,t) = \frac{\partial \psi_{fsp}}{\partial x}(x,h,t)$, ψ_{fsp}, given by the solution of the form (19) of the flow problem without a wave breaker. (54)

According to the previously determined solution, we obtain that:

$$u_{fsp}(x,t) = -at + \sum_n u_{nfsp}(x,t), t \in [0, t_1]; \quad (55)$$

$$u_s(x,t) = -at_1 + \sum_n u_{n\,fsp}(x,t), t \in [t_1, t_s]. \quad (56)$$

$$u_{n\,fsp}(x,t) = K_n \lambda_n ch(\lambda_n H)\sin\left(\lambda_n (x+l)\right) sin(\omega_n t), t \in [0, t_s],$$

(see [CHO16]). (57)

Under conditions (48)-(51), C represents the inertia coefficient and is negligible if the thickness of the stopper is neglected and $\alpha = \left(\frac{1}{PC} - 1\right)^2$, (see [POG19]), is a coefficient that takes into account the porosity of the wave breaker. $f(t) = \int \frac{F}{m} dt = f_0 t$, F the force distributed on the breaker (taking into account the initial speed U_0, the volume of liquid in the tank (i.e. the height of the liquid in the tank, H).

Hydrostatic pressure and free surface can be described by:

$$p = -g\frac{\partial \psi}{\partial t}, \eta = \frac{p}{\rho g}. \quad (58)$$

Tab. 6.1. Parameter values f_0 [N/kg] relative to the initial speed U_0

Volume liquid [L]	Mass[kg]	f_0 for U_0=10km/h	f_0 for U_0=30km/h	f_0 for U_0=50km/h
15	12.5	2,00800	2,28800	2,57600
25	20.9	2,00000	2,27751	2,56459
35	29.2	2,00342	2,28082	2,57192
45	37.6	2,00000	2,27926	2,56915

The values in Table 6.1. were obtained on the basis of the data in Tables 5.2 and 5.3 corresponding to Chapter Five. These values will be used in the graphs shown in fig. 6.2-6.7, the parameter f_0 interference in the relationship (48). Parameter f_0 calculated according to Force F (in Table 5.3) at the preset speed (10, 30, 50km/h of tab 5.3) and the mass of the liquid in the tank.

Note the solutions of the current function in the two areas :

$$\psi^1 = \psi_0^1 + \psi_f \ (\mathrm{x}\epsilon[-l,0]), \text{ respectively } \psi^2 = \psi_0^2 + \psi_f \ ,(\mathrm{x}\epsilon[0,l]), \tag{59}$$

with: $\psi_f = \sum_{n=1}^{\infty} \psi_n \, \psi_n(x,y,t) = f_n^1(\mathrm{x},\mathrm{y}) \sin(\omega_n^{sp}\mathrm{t})$, solution type (19) with $n \geq 1$,

$$f_n^1 = -C_n \cos\left(\lambda_n^{sp}(x+l)\right) ch(\lambda_n^{sp} y), \tag{60}$$

with:

$$\lambda_n^{sp} = n\pi/l, \left(\omega_n^{sp}\right)^2 = g\lambda_n^{sp} \, \mathrm{th}\left(\lambda_n^{sp} H\right) \tag{61}$$

f_n^1 fundamental solutions that verify:

$$\Delta f_n^1 = 0, \frac{\partial f_n^1}{\partial x}(-l,y) = 0 = \frac{\partial f_n^1}{\partial x}(0,y), \frac{\partial f_n^1}{\partial y} = 0|_{y=0}. \tag{62}$$

and ψ_0^1 and ψ_0^2 are solutions that verify (20).

thus, $\forall y \in [h, h+h_{sp}]$, for $t \in [0,t_1]$,

$$\psi_0^1 = A_{01}^1(t) + \frac{1}{\omega_1^{sp}}\left[\int_0^1 -a(1-\theta) + f_0\theta d\theta\right] + \mathrm{x}((U_0 - at)(1-\theta) + f_0 t\theta),$$
$$\mathrm{x}\epsilon[-l,0] \tag{63}$$

,

and

$$\psi_0^2 = A_{01}^2(t) + \frac{1}{\omega_1^{sp}}\left[\int_0^1 f_0(1-\theta) - a\theta d\theta\right] + \mathrm{x}(f_0\mathrm{t}(1-\theta) + (U_0 - at)\theta),$$
$$\mathrm{x}\epsilon[0,l], \theta = \frac{t}{t_1}, \tag{64}$$

for $t \in [t_1, t_s]$,

$$\psi_0^1 = A_{02}^1(t) + \mathrm{x}((U_0 - at)(1-\theta) + f_0 t\theta), \mathrm{x}\epsilon[-l,0], \tag{65}$$

and

$$\psi_0^2 = A_{02}^2(t) + \mathrm{x}(f_0\mathrm{t}(1-\theta) + (U_0 - at)\theta) \ , \mathrm{x}\epsilon[0,l], \ \theta = \frac{t-t_1}{t_s - t_1} \tag{66}$$

In which :

$$A_{01}^2(t) = A_{01}^1(t) = c_{11}e^{r_1 t} + c_{12}e^{r_2 t}, \ A_{02}^2(t) = A_{02}^1(t) = c_{21}e^{r_1 t} + c_{22}e^{r_2 t}, \tag{67}$$

considered a mediation of the variation over time of the initial impact.

The free surface , fig.6.5, will be determined by the relationship $\frac{\partial \psi}{\partial t} + g\eta = 0, y = \eta$ (68)

$$\eta_0^1 = -\frac{1}{g}\frac{\partial \psi_0^1}{\partial t} - \frac{1}{g}\frac{\partial \psi_f}{\partial t}, \eta_0^2 = -\frac{1}{g}\frac{\partial \psi_0^2}{\partial t} - \frac{1}{g}\frac{\partial \psi_f}{\partial t}, \quad (69)$$

Cu : $-\frac{1}{g}\frac{\partial \psi_f}{\partial t} = \frac{\omega_n^{sp} C_n}{g}\sum_{n=1}^{\infty}\cos\left(\lambda_n^{sp}(x+l)\right) ch(\lambda_n H)\cos\left(\omega_n^{sp} t\right), \quad (70)$

$$C_n = \frac{gH}{\omega_n^{sp} ch(\lambda_n^{sp} H)}. \quad (71)$$

For $t \in [0, t_1]$:

$$-\frac{1}{g}\frac{\partial \psi_0^1}{\partial t} = -\frac{1}{g}[\dot{A}_{01}^1(t) + x\left(-a + 2(f_0 + a)\frac{t}{t_1} - \frac{U_0}{t_1}\right)], \quad (72)$$

$$-\frac{1}{g}\frac{\partial \psi_0^2}{\partial t} = -\frac{1}{g}\left[\dot{A}_{01}^2(t) + x\left(f_0 + \frac{U_0}{t_1} - 2(f_0 + a)\frac{t}{t_1}\right)\right] \quad (73)$$

For $t \in [t_1, t_s]$:

$$-\frac{1}{g}\frac{\partial \psi_0^1}{\partial t} = -\frac{1}{g}[\dot{A}_{02}^1(t) + x\left(-a + 2(f_0 + a)\frac{t}{t_s - t_1} - \frac{U_0}{t_1}\right)], \quad (74)$$

$$-\frac{1}{g}\frac{\partial \psi_0^2}{\partial t} = -\frac{1}{g}[\dot{A}_{02}^2(t) + x\left(f_0 + \frac{U_0}{t_1} - 2(f_0 + a)\frac{t}{t_s - t_1}\right)]. \quad (75)$$

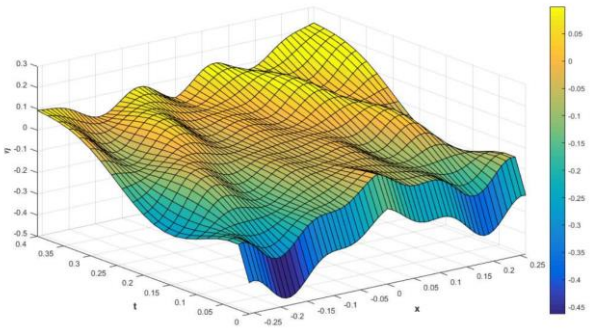

Fig.6.5a. Evolution of the free surface with baffle ($\eta(x,t) = \eta_0(x,t) + \sum_n \eta_n(x,t)$ [m]) in the two areas of integration, t=0.4s, according to the (69), (72), (73)

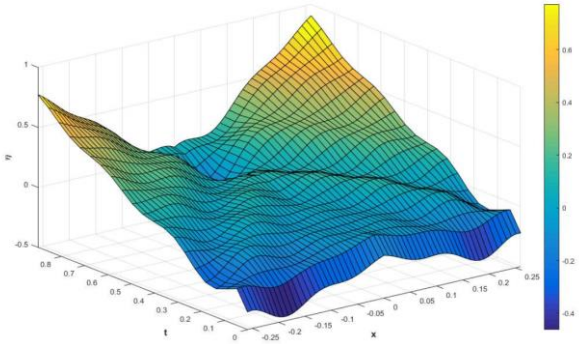

Fig.6.5b. Evolution of the free surface with burglar in the two areas of integration, t=0.9s according to relations (69), (72) - (75)

According to Fig.6.5, in the case of a tank with a breaker, a single wave appears, but larger, and the liquid tends to go to the sides. Theoretically, it is good to integrate a slosh noise baffle into a tank because the noise generated by the blinking phenomenon is diminished in terms of the lack of waves.

In conclusion, it is observed from the two figures, fig. 6.6 and fig. 6.7, that the free surface has totally different behavior, the number of waves decreased considerably in the case of integration of a baffle solution, and thus the discomfort caused by the blinking phenomenon will be reduced.

Negative values on the X axis are due to the axis system considered, so -0.25m and + 0.25m are the tank walls.

Take as reference (zero) surface described by the level of the liquid at rest. Positive and negative variations from the reference level after braking.

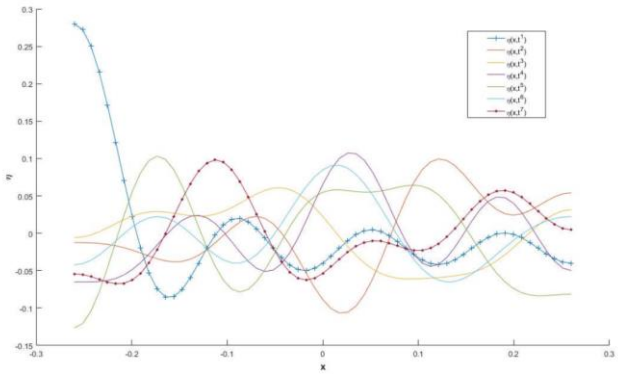

Fig. 6.6a. Evolution of wave amplitude (section of the free surface in direction X) for a tank without a burglar, according to relations (33) and (34)

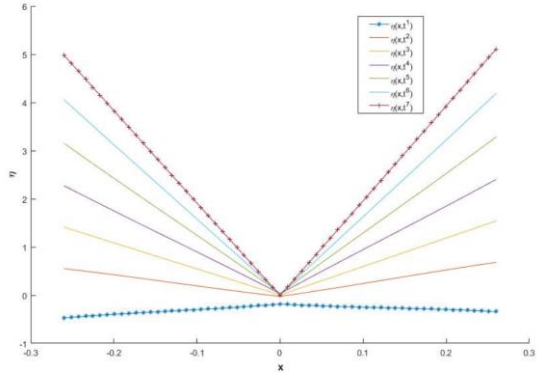

Fig. 6.6b. Evolution of wave amplitude (free surface section in direction X) of waves for a breaker tank according to relationships (69), (72)-(75)

As can be seen in fig. 6.7.b ripples of the free surface occur, these being unfractionated surfaces (the gradient on the curves on the surface curves does not change convexity), smoother, and thus no noises are generated by the collision of small waves. The greater the distance between two peaks of amplitude, the more flattened, noise-free disputer the free surface is.

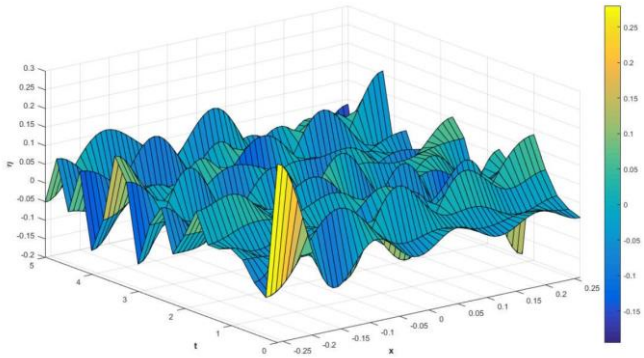

Fig.6.7.a. Behavior of the free surface for a slosh noise baffle -free tank according to relationships (33) and (34)

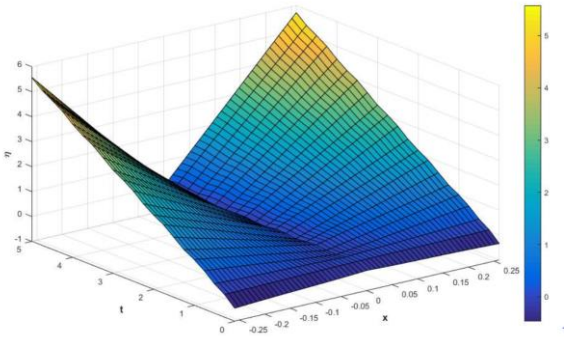

Fig.6.7.b. Behavior of the free surface for a slosh noise baffle in the tank, according to relationships (69), (72)-(75)

In the model considered, the study is carried out in the center of the tank, not taking into account that we have a higher limitation given by the ceiling of the tank. In the case of future research, the study is advanced taking into account the limitation of the model at the top, considering that the wave returns, the potential movement becoming turbulent.

For the graphs in figures 6.5, 6.6 and 6.7, an own computing code was created in MatlabR2016.R, as detailed in the thesis.

6.4. Future research prospects. Future calculations:

Using Bernoulli's integral we have the correspondence:

$$\frac{1}{2}\left(\mathrm{v}_{fsp}\right)^2+\frac{c^2{}_{fsp}}{\gamma-1}=\frac{1}{2}\left(\mathrm{v}_{sp}\right)^2+\frac{c_{sp}^2}{\gamma-1}. \quad (76)$$

where c_{sp}^2 is the sound speed in second case and $\left(\mathrm{v}_{sp}\right)^2=\left(u_{sp}\right)^2+\left(v_{sp}\right)^2$. (77)

$$u_{sp}^1=\frac{\partial\psi_0^1}{\partial x}=(U_0-at)(1-\theta)+f_0t\theta)+\sum_{n=1}^{\infty}\frac{C_n}{\lambda_n^{sp}}\sin\left(\lambda_n^{sp}(x+l)\right)ch(\lambda_n^{sp}y),$$
$$\theta=\frac{t}{t_1}, \quad (78)$$

$$v_{sp}^1=\frac{\partial\psi_0^1}{\partial y}=-\sum_{n=1}^{\infty}\frac{C_n}{\lambda_n^{sp}}\cos\left(\lambda_n^{sp}(x+l)\right)sh(\lambda_n^{sp}y),\forall y\in[h,h+h_{sp}],$$
$$t\in[0,t_1]; \quad (79)$$

$$u_{sp}^2=\frac{\partial\psi_0^2}{\partial x}=f_0\mathrm{t}(1-\theta)+(U_0-at)\theta+\sum_{n=1}^{\infty}\frac{C_n}{\lambda_n^{sp}}\sin\left(\lambda_n^{sp}(x+l)\right)ch(\lambda_n^{sp}y),$$
$$\theta=\frac{t-t_1}{t_s-t_1} \quad (80)$$

$$v_{sp}^2=\frac{\partial\psi_0^2}{\partial y}=-\sum_{n=1}^{\infty}\frac{C_n}{\lambda_n^{sp}}\cos\left(\lambda_n^{sp}(x+l)\right)sh(\lambda_n^{sp}y),\forall y\in[h,h+h_{sp}],$$
$$t\in[t_1,t_s] \quad (81)$$

Potential energy:

$$U^e=\frac{1}{2}\rho gb\left(\int_{-l}^{0}(\eta_0^1)^2(\mathrm{x},t)\,d\mathrm{x}+\int_0^l(\eta_0^2)^2(\mathrm{x},t)\,d\mathrm{x}\right),\qquad t\in[0,t_s], \quad (82)$$

Kinetic energy : $T^e=\frac{1}{2}\rho\int_V(\nabla\psi)^2\,dV.$ (83)

Potential energy is to be analyzed in both cases.

However, the results obtained in the modeling carried out so far are totally original, the dependencies highlighted by the motion equations having a worldwide novelty character.

CHAPTER 7: Functional analysis - acoustic tests using variants of slosh noise reduction systems inside a fuel tank under real conditions

7.1. General considerations of analysis

The analysis aims to study the noise level generated by breaking waves into a vehicle tank and the influence of a slosh noise baffle embedded in the tank on reducing it. A prototype analysis shall be considered to simulate the behavior of the liquid in the tank and to record data on the noise caused by it.

Following the previous decision to abandon a constructive variant, only two models of slosh noise baffles will be studied. For the purpose of physical testing, the 3D models of the two baffles were considered and prototypes for each model were made (Fig. 7.1. , Fig. 7.2.).

Fig. 7.1. Link Baffle assembled in fuel tank

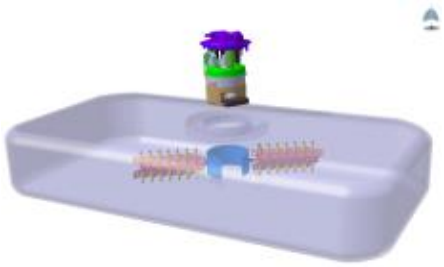

Fig. 7.2. Fishbone baffle assembled in fuel tank

The following parameters shall be considered for the purpose of the study:

- The amount of liquid inside the tank : 15L, 25L, 35L, 45L;
- Vehicle speed: 10km/m, 30km/h;

In order to carry out functional analysis and acoustic tests, prototype parts were made for the two technical solutions of baffles as well as for the generic tank presented in the thesis.

The prototypes of the two slosh noise baffles were made using 3D printing FD01 technology. Due to technical limitations, a material other than the recommended one was used. The material used to make prototypes is ECOMAX PLA – polylactic acid. This is a premium material used for 3D printing of prototypes of various components, a semi-crystalline resin with high mechanical properties.

The static analysis of these concepts was carried out considering a different material, Polyamide 6+PP, so there will be differences in the functional analysis due to the different properties of the two materials mentioned. Table 6.1 shows some of the mechanical characteristics of the material used for 3D printing of the two technical wave breaker solutions, compared to the mechanical properties of Polyamide that was used in numerical simulations – treated in Chapter 5.

Tab. 7.1. Mechanical properties of the material Polyamide 6 +PP vs. ECOMAX PLA [ULP15]

Mechanical properties	Polyamide 6+PP	ECOMAX PLA
Density	1.26 g/cm^3	1.24 g/cm^3
Traction resistance [MPa]	200 MPa	56 MPa
Break resistance, yield [MPa]	140 MPa	34 MPa
Breaking elongation	500 %	8 %

It can be seen in Tab. 7.1 that the material used for 3D printing provides lower breaking resistance as well as lower elasticity. The test will be carried out using this material due to the financial limitation of the project, the noise level analysis is not influenced by these parameters, there is only the risk of interruption of the test due to the risk of breaking the slosh noise baffle prototype.

7.2. 3D printing

In order to carry out the acoustic tests on prototype parts, a fuel tank was carried out considering a simplified, cuboid form based on the dimensions presented in Chapter 1 of the paper.

Several simple constructive solutions have been adopted to adapt to the vehicle used for testing. Thus, the tank was built of 10mm plexiglass plates, transparent so that the movement of the liquid inside is easily viewed by the observer and the associated camera. It was placed on a melamine PAL plate to make it as simple as possible to catch it by the vehicle to be used for physical tests (fig. 7.3).

Fig. 7.3. Simplified fuel tank

In order to present the introduction of baffle into the tank mounted in the final position, a 140mm hole was made in the tank ceiling. This is carried out according to the outer size of the pump Fuel Delivery Module flange, (Fig. 7.4).

Fig. 7.4. Detail Simplified fuel tank – module fixing straps

Starting from the simplified 3D models of wave breakers, the prototype parts used for physical testing were made. The production of these parts was carried out with the help of 3D printers belonging to the Polytechnic University of Bucharest – Faculty of Industrial Engineering and Robotics, Product Development Laboratory. Thus, the following sub-components were:

1. Lower body Fuel Delivery module(Fig. 7.5);
2. Central body for lower fixing of module columns (Fig. 7.6, Fig.7.7, Fig. 7.8)

Fig. 7.5. Body Fuel Delivery module

Fig. 7.6. Central housing– top view

Fig. 7.7. Central Housing

Fig. 7.8. Central housing for lower attachment of module columns – side view

3. Columns Fuel Delivery module x 3 pieces (Fig.7.9);
4. Upper flank Fuel Delivery module (Fig. 7.10, Fig. 7.11, Fig. 7.12);

Fig. 7.9. Columns

Fig. 7.10. Upper flange– overview

Fig. 7.11. Upper Flange – Bottom View

Fig. 7.12. Upper Flange – Top View

5. Link Structure (Fig. 7.13);
6. Fishbone module structure (Fig. 7.14);
7. Adjacent Cylinder (Fig. 7.15)

Fig. 7.13. Link structure

Fig. 7.14. Fishbone module structure

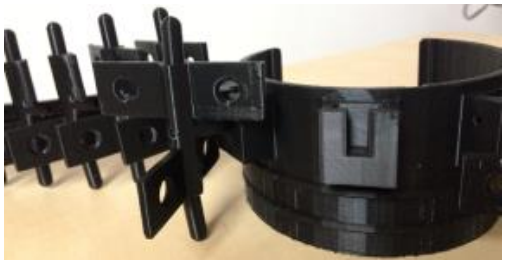

Fig. 7.15. Adjacent cylinder and attachment of fishbone structures to it

As can be seen from Fig. 7.16-18, the assembly of 3D printed parts that form the Fuel Delivery module assembly to be used in all acoustic tests has been carried out. It was also checked that the module is fixed within the tank by correctly positioning the clamps on the upper face of the Fuel Delivery module flange.

Fig. 7.16. Fix column on Fuel Delivery module

Fig. 7.17. Fuel Delivery module

Fig. 7.18. Detail grip flange upper Fuel Delivery module through the two straps

The assembly of these parts was carried out using self-locking pins, and a 2mm diameter steel cable passed through the holes of the Links and adjacent cylinders. (Fig. 7.19).

Fig. 7.19. Assembly details Link baffle

The prototype of the Fishbone slosh noise baffle was carried out using the same method of making subcomponents as in the Link slosh noise baffle, i.e. 3D printing.

Fig. 7.20. Assembly details Fishbone baffle

The assembly was done by directly joining the parts through the T-type channels according to the design, as can be seen in the Fig. 7.20.

7.3. Definition of test method and test scenario

To date, no standard method of recording the noise level produced by the slosh noise phenomenon has been based, so, within the thesis, a method of own has been created to record the noise level and to study the influence of the introduction of slosh nose baffle on it. The method will form the basis of the experimental research on the recording of the noise level as perceived by the driver of a motor vehicle. Thus, the testing included the design of two stages: (1) the construction and installation of a prototype tank in a vehicle and the recording of noise, carried out with a standard device. Thus, a variant of testing and recording of data has been defined that can also be used in similar subsequent research.

To carry out the proposed tests, the prototype tank is fixed to a frame and mounted inside a Dacia-branded vehicle, Model Lodgy. As shown in Fig. 7.28, a frame is mounted above the tank to be used to support the decibel level recording device. The device is located at a height of 500mm above the tank and is maintained in the same position by the supporting frame. This eliminates the variation in the distance, position and movement of the recording device (Fig 7.21).

Fig. 7.21. Prototype tank mounted in the vehicle

Noise recording was done using an Iphone brand smartphone, model 5S, using the BOSCH iNVH version 1.1. The application is specially developed by Engineers at Robert Bosch for measurements of vibrations and noise inside vehicles and the detection of noise sources in them during field tests by simple use with the help of a smart device.

Tests will be made using as input parameters in the analysis:
- the amount of liquid in the tank: 15l, 25l, 35l, 45l;
- vehicle speed: 10km/h, 30km/h
- absence or presence of a slosh noise baffle inside the tank.

In order to make a set of records as conclusive as possible, the physical tests were carried out in a closed space which ensured a run of the vehicle at a speed of up to 30 km/h and sufficient braking space. Thus, a warehouse with a running length of about 120m was chosen, with asphalt road surface. The test in this space ensured a minimal influence of external noise factors.

7.3.1. Recording data on noise variation in a slosh noise baffle-free tank

The initial test was performed by recording the noise level at rest (with the engine off), the lack of movement in the tank and no other external factors existing. This measurement is carried out to identify the level of background noise perceived by the device used. Variations can be observed around 31 dB.

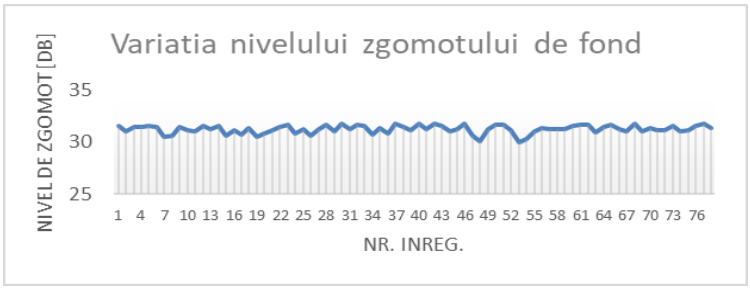

Fig. 7.22. Variation in background noise level

RESULTS	
Sampling Frequency = 44100.000000	
BlockSise = 4096.000000	
Window = Hanning	
Weighting = A Weighting	
Averaging = Instantaneous	
MinFrequency =20	
MaxFrequency = 20000	
Time [s]	OverallLevel [Db]
0.0	32
0.1	31
0.2	31
0.3	31
0.4	32
0.5	31
0.6	30

Fig. 7.23. Excerpt from Bosch app

In Fig. 7.23. results extracted from the Bosch INVH app are presented.

Case "S1" is the vehicle's 10 km/h run before braking, using 15L of liquid in the prototype tank. In Fig. 7.24 we can see the behavior of the waves produced at the time of braking.

Fig. 7.24. Case S1 with 15L of liquid, without baffle

The test was intended to record the level of decibels (Y-axis) throughout its duration, and on the basis of the recorded data, the analysis of the efficiency of some baffles in terms of the noise level produced.

In the graph in Fig. 7.25, you can see the recording of the raw simulation data. Also, within this graph, the macro-level of the analysis could be identified the times of the increase and decrease in the decibel level, thus:

A. Red Area – represents the start of the engine and the acceleration of the vehicle;
B. Blue Area – represents the time of braking of the vehicle;
C. Orange Area – represents the time of engine shutdown (option Start/Stop);
D. Green Area – represents the moment of total rest of the vehicle, basically the background noise and noise made by the free movement of the waves in the tank.

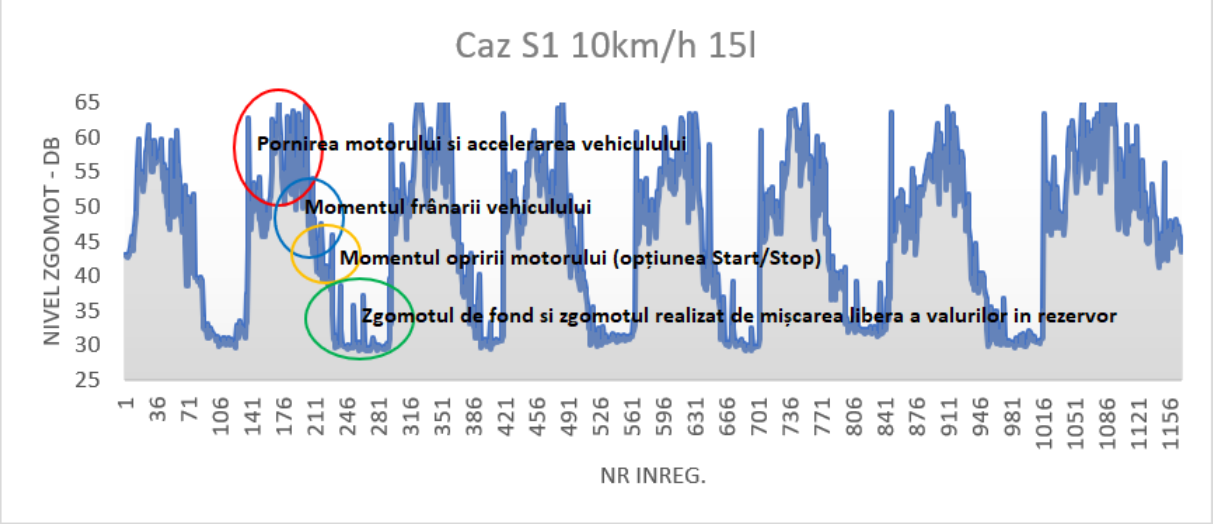

Fig. 7.25. Test graph S1

Simulations and recording of data on the cases described (running at 10km/h and 30 km/h with a quantity of 15l, 25l, 35l, 45l) without a wave breaker mounted in the tank, are found in detail in the doctoral thesis.

7.3.2. Recording of noise level variation data in a tank equipped with a Link baffle

The tests will be carried out using the same method as in the previous case, after the introduction of the Link baffle into the tank, as can be seen in Fig. 7.26 and Fig. 7.27.

Fig. 7.26. Link slosh noise baffle

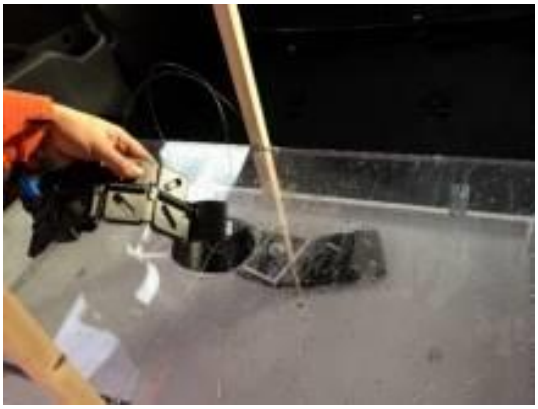

Fig. 7.27. Link Baffle introduced in tank

The prototype test shall be carried out using the same steps as in the case of the test carried out without the presence of a baffle. Thus, for the first case, 'Z1', the amount of liquid of 15L and a run of the vehicle of 10 km/h was used. In fig7.28 can be observed the way the liquid moves to the front of the fuel tank at braking moment. The wave that is formed can be observed.

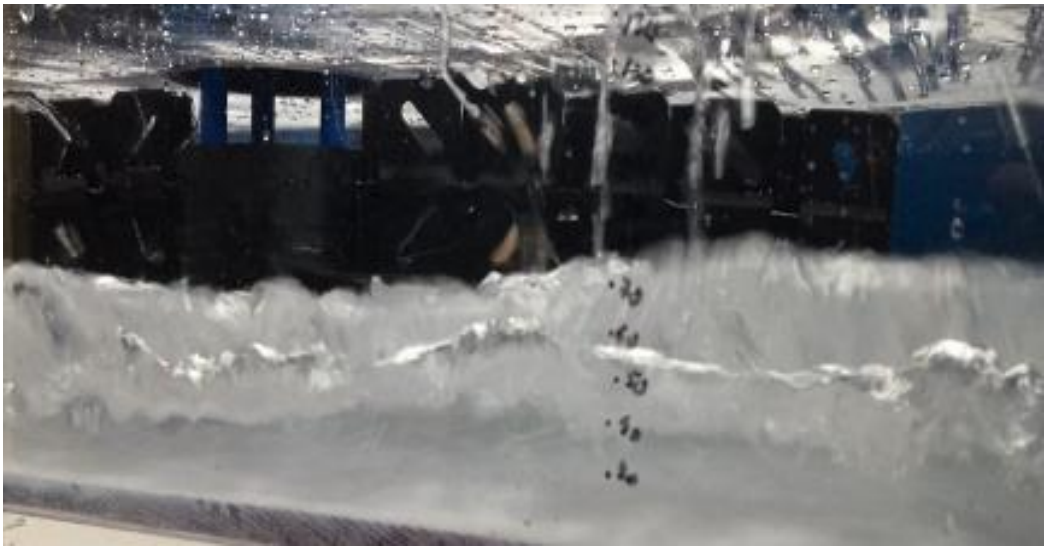

Fig. 7.28. Caz Z1 – Wave generation in the tank during braking moment

The result of the noise level test can be seen in the graph in Fig. 7.29. A decrease in noise variation (green area) can be seen on the graph, but the comparative analysis is shown in the thesis. The graph identifies the same 4 areas described in Chapter 7.3.1. thus:

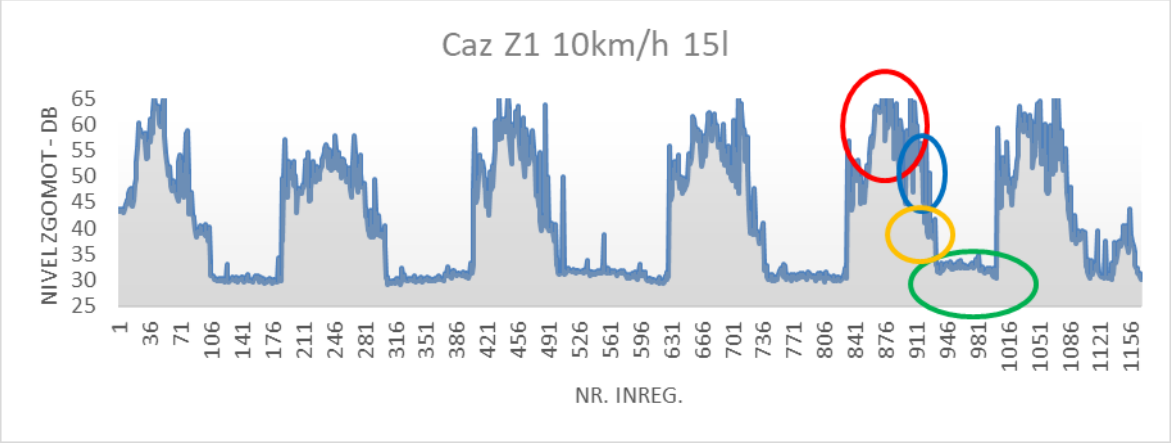

Fig. 7.29. Graphic test Z1

The simulations and recording of the data on the cases described (running at 10km/h and 30 km/h with a quantity of 15l, 25l, 35l, 45l) using the Za wave breaker mounted in the tank, are found in detail within the doctoral thesis.

7.3.3. Recording of noise variation data in a tank equipped with Fishbone slosh noise baffle

The tests shall take place under the same conditions as those in sub-chapter 7.3.2, the only variable added being the Fishbone baffle, Fig. 7.30.

As can be seen in Figure 7.30, the baffle is easily inserted into the tank through the tank hole intended for the Fuel Delivery module, Fig. 7.31. Then insert the Fuel Delivery module into the tank while fixing the wave breaker.

Fig. 7.30. The Fishbone baffle s inserted into the tank through the tank hole intended for the

Fig. 7.31. The Fuel delivery module is positioned in the tank while also fixing the wave breaker

Testing of the prototype is carried out using the same steps as in previous cases. Thus, the first simulation, "F1", was carried out using 15L of liquid (Fig. 7.32) and a vehicle run of 10km/h. In Fig. 7.33, the graph showing the variation in the decibel level in this test is presented.

Fig. 7.32. Case F1 – Wave formation in the tank at braking time

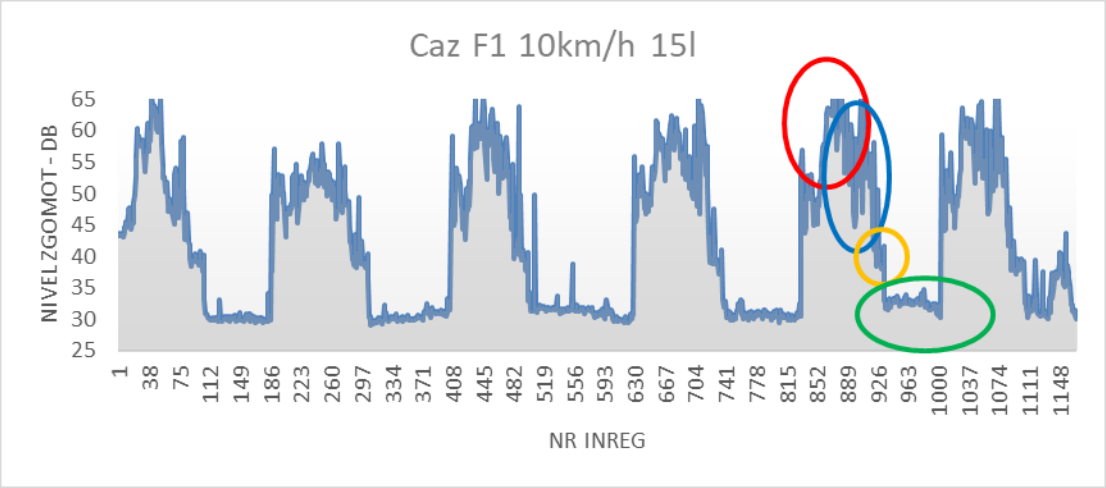

Fig. 7.33. F1 Test Chart

Similar behavior can be observed as in the case of the Link baffle. This identifies the same four areas described in subchapter 7.3.1.

The simulations and recording of the data on the cases described (running at 10km/h and 30 km/h with a quantity of 15l, 25l, 35l, 45l) using the Fishbone baffle mounted in the tank, are found in detail within the doctoral thesis.

7.4. Interpretation of noise variation

In order to analyses the data obtained from physical tests, it was considered to filter the data from the graphs obtained according to the following observations:

- noise level: 29-31dB - record when the engine is switched off and only background noise is recorded;
- noise level: 42-45dB – recorded at the time of braking and stopping the engine;
- noise level variation: 29-45dB - recorded after the engine shutdown represents background noise and noise produced by waves formed in the tank;
- Only 18 cases of the 24 previously proposed will be analyzed due to lack of records in the case of the use of the Za wave breaker at 45L (details in head 7.3.2. in the doctoral thesis)

In order to determine the efficiency of the introduction of a slosh noise baffle into the tank and to reduce the level of "slosh noise" noise, the records of the cases presented shall be analyzed. This will

analyses the variation in the noise recorded after the engine has stopped until the background noise is recorded.

To carry out a classification of the three groups of cases, the averages of the recorded noise values (decibels), their variation and their distributions will be compared.

To carry out this comparative analysis of the noise level recorded in the case of the tests carried out, as well as to establish the statistical basis for comparison on the effect on the noise level following the use of a slosh noise baffle, a standard graphic report of each test will be made using an equal number of records for each case.

This summary graphic report is made with the help of the software application for statistical calculation, Minitab - a software developed by Pennsylvania State University since 1972. [MIN20],[MIC18].

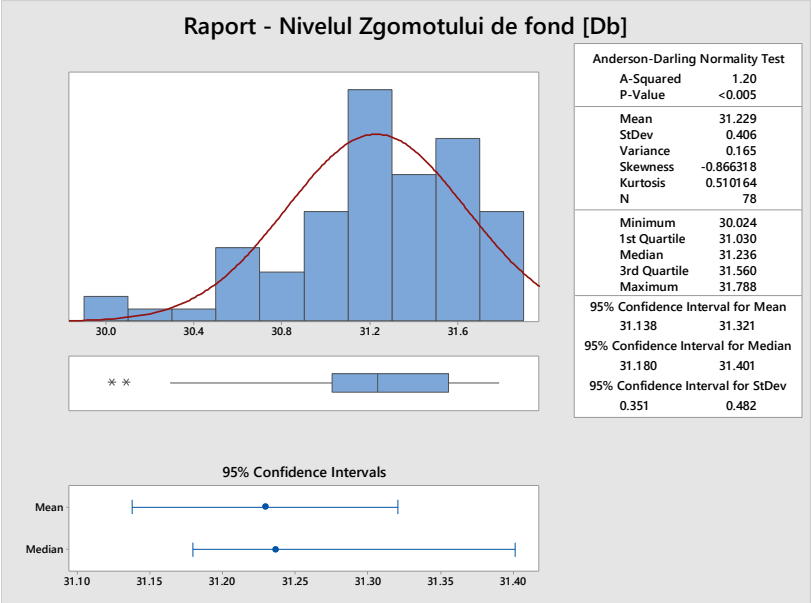

Fig. 7.34. Summary report

The median and the average both measure the central trend, but "unusual" values, called extreme values, can affect the median less than the average affects. If the data is symmetrical, the average and median will have the same value. In the experimentally measured data, it can be observed that the average is 31.2dB and the Median is equal to 31.22dB. This may indicate that we do not have unusual values in the data string [MIN20],[MIC18], [ILI09].

Standard deviation is one of the most common parameters for measuring dispersion, indicating the degree of scattering of data relative to the mean. The natural or random variation of a process can also be called noise. In the case of background noise level analysis, a relatively low standard deviation value can be observed, with 0.46dB considering the average of 31.2dB [ILI09].

In the case studied, the background noise level shows a negative asymmetry, most values being around the average of 31.2dB, a small number of records being oriented to the left around 30dB values.

Extreme values are those values in data that are at a great distance from other values and can strongly influence the outcome of the analysis. In the case of our analysis, such data in the extreme range represent noise values that are considered noises produced by the waves in the tank. In the background noise level data, it can be observed that there are no such [ILI09].

7.5. Comparative analysis of data on the variation in decibel levels in the cases studied

Considering the same method of analysis as in the case of background noise, the data taken specific to the 3 cases studied previously were analyzed. The doctoral thesis contains the data and analysis of the 18 simulations considered. The results of this analysis can be found in Table 7.2.

Tab. 7.2. Centralization of data on the variation in decibel levels in the three cases studied

Crt. No.	Case	Average [dB]	Dispersion [σ^2]	Median	Quartile 1	Quartile 3	Difference (Q3-Q1)
1	F3	30.75	7.9	30.75	29.73	30.27	0.54
2	Z2	31.81	11.454	30.46	30.075	31.115	1.04
3	Z1	31.12	2.26	30.89	30.465	31.259	0.794
4	F4	31.95	18.47	29.96	29.5	31.3	1.8
5	Z6	31.8	7.29	30.97	30.63	31.59	0.96
6	Z5	31.67	6	30.8	30.3	31.84	1.54
7	F1	32.25	15.23	30.71	30.23	31.98	1.75
8	Z4	32.08	6.2	31.26	30.79	32.35	1.56
9	F6	32.43	15.6	30.77	30.3	32.4	2.1
10	F2	33.14	15.24	31.62	30.99	32.72	1.73
11	F5	32.39	9.5	31.4	30.6	32.86	2.26
12	Z3	32.446	11.02	30.84	30.29	33.36	3.07
13	S3	33.69	19.46	31.48	30.92	34.62	3.7
14	S2	34.606	10.8	33.55	32.149	36.43	4.281
15	S4	33.95	21.48	31.34	30.85	38.58	7.73
16	S1	33.15	22.75	30.08	29.77	38.617	8.847
17	S6	34.47	28.07	31.5	30.7	39.18	8.48
18	S5	40.48	43.3	37.55	35.24	45.43	10.19

It can be observed that in cases of non-use of a slosh noise baffle (S1-S6), we find higher values for all characteristics. In the table was performed sorting by increasingof the value of recorded data by Quartile 3, which characterizes the highest 25% of the recorded values.

The difference (Δ) represents the difference between the largest 25% of the recorded values – Quartile 3 – and the lowest 25% of the recorded values – Quartile 1 –. The difference (Δ) can be considered the most effective parameter for interpreting the noise variation caused by the breakage of waves in the tank. The study was carried out to determine the noise variation caused by the breakage of waves in the tank when stopping any other disruptive factor.

Quartile 1 values are located between 29-32dB for most tests. Thus, it can be said that in the case of tests, the highest amount of the first 25% of the recordings is confused with the background noise.

According to Quartile 3 values, a considerable difference can be observed between the test performed without slosh noise baffle and the tests carried out with the two baffles. Thus, the maximum value of the first 75% of the recorded values is between 34.6dB and 45dB in the case of non-use of a slosh noise baffle. With the introduction of baffles, Quartile 3 values decrease, thus the values between 30.27dB and 33.36dB are observed.

Lower Difference (Δ) values can be observed when using a baffle 0.54dB – 3.07dB, while if a baffle is not used, the difference (Δ) increases depending on the case studied 3.7dB – 10.19dB. It can be interpreted as a decrease in the noise level produced by the waves in the tank with baffle is used.

Tab. 7.3. Centralization of tested cases

Crt. No.	Case	Average [dB]	Dispersion [σ2]	Median	Quartile 1	Quartile 3	Difference (Q3-Q1)
1	S	35.06	30.1	32.79	30.89	38.87	7.98
2	Z	31.82	7.4	30.85	30.43	31.78	1.35
3	F	32.156	14.01	30.71	30.05	32.28	2.23

According to data centralization, the following observations can be made in Tab. 7.3:

- Introducing a slosh noise baffle reduces the average decibel values recorded from 35dB to 32dB;
- The difference in recorded values (decibels) decreases from 8dB to 1.3dB in the case of the introduction of the Link baffle ;
- The dispersion of recorded noise values (decibels) decreases from 30.1dB to 7dB when using the Link baffle;
- The differences between the cases of the use of the two slosh noise baffles, Mean, Median and Dispersion of the recorded decibel values showing similar behavior when using one of the two slosh noise baffles.

According to the functional analysis carried out by testing the two prototypes in a tank, a decrease in the noise level, identified as a slosh noise phenomenon, can be observed.

CHAPTER 8: General conclusions, personal contributions, dissemination of results, future research directions

8.1. General conclusions

The doctoral thesis entitled " Research on development of slosh noise baffles for automotive fuel tanks" presents the research undertaken by the author on the development of innovative technical solutions of integrated and adaptable wave breakers in existing fuel tanks in order to improve the phenomenon of slosh noise, by shaping the dynamic behavior of the fuel in the tank. Moreover, this was the very main objective of the thesis.

The general conclusions of the research carried out are as follows:

1. The wing wave breaker has a wing deformation of 2300mm and a risk of breaking the wings, the largest deformation of the three concepts analyzed. It also presents a risk of breakage, the material being able to yield at 180 MPa considering the application of a force of 100 N perpendicular to the wings. The Wing Wave Breaker has the greatest deformation of the wing under normal operating conditions >13mm. For the reasons listed above, it did not pass the stage of making the prototypes and confirming the results by carrying out the physical tests. This concept has been abandoned from research point of view.

2. Under normal conditions of use, the “link” wave breaker will withstand breakage and can change its shape/position by up to 35mm.

3. The Fishbone wave breaker shows the slightest deformation of the wing under normal operating conditions <5mm;

4. For use under extreme conditions it is recommended to use a material with polypropylene-like properties, but with a breaking resistance >100 MPa;

5. From mathematical point of view, it was carried out to transpose the phenomena of movement of fluid inside the tank, representing both the waves produced and the braking phenomenon associated with the slosh noise effect, into mathematical and analytical models. These allowed mathematical modeling of the free surface of the fluid under the hypothesis that we do not have a solution for breaking the waves inside a tank, compared to the situation where we encounter the slosh noise solutions integrated into the tank. Thus, it emerged that the amplitude of the movement of the free surface of the fluid in the case of the implementation of an anti-slosh noise solution of the type of baffle is reduced by half compared to the movement of the free surface of the fluid contained in a baffle free fuel tank that.

6. For “Link” type baffle and fishbone wave breakers, the analysis continued with physical tests demonstrating the effectiveness on the modelling of the dynamic fuel behavior in the vehicle tank, as well as the representativeness of the numerical simulations performed. In addition, the risk of rupture within the link wave breaker was confirmed by physical tests.

7. Introducing a wave breaker reduces the average decibel values recorded from 35dB to 32dB;

8. The difference in recorded decibel values decreases from 8dB to 1.3dBb in the case of the introduction of a the link wave breaker;

9. The variation in recorded decibel values decreases from 30dB to 7dB when using a link wave breaker;

10. The differences recorded between the cases of the use of the two types of wave breakers are small, with Media, Mediana and Difference in decibel values showing similar behavior when using one of the two types of wave breakers.

The implementation of any wave-breaking solution between the two studied (link type or fishbone type) shows a noticeable improvement in terms of generated noise, as can also be seen in Figure 8.1.

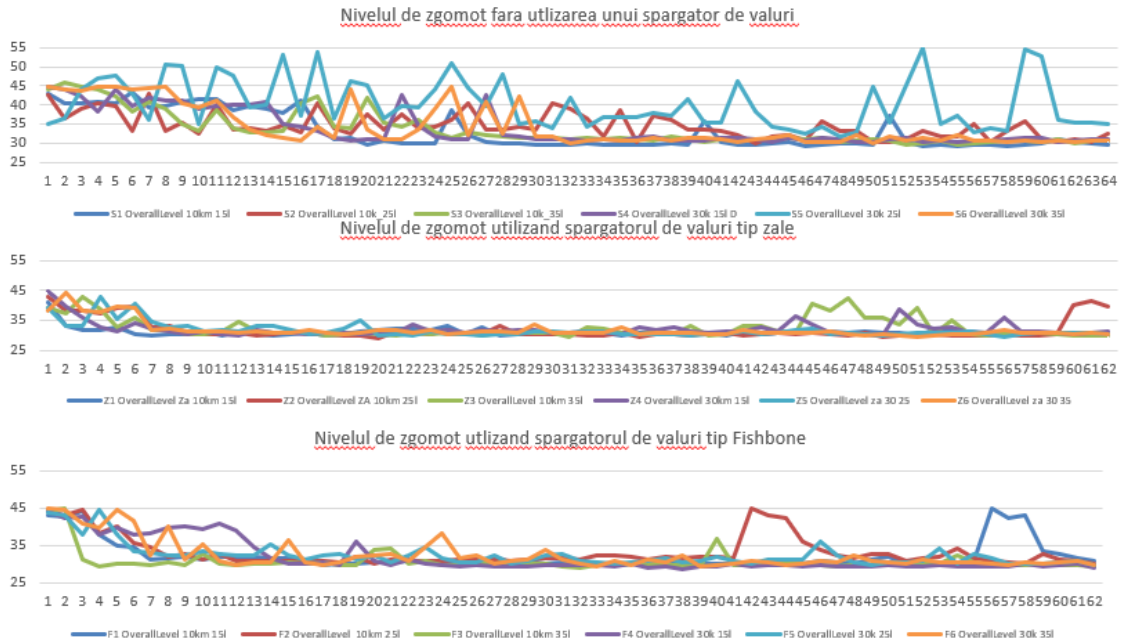

Fig.8.1. Variation of noise level depending on the technical solution of slosh noise baffle implemented

8.2. Personal contributions

Following the research presented, the author made personal contributions to the field of modeling the dynamic behavior of the fuel inside the tank of a vehicle by:

1. Realization of the bibliographical study on the current state of the art of the tanks in terms of manufacturing technologies, fuel trend and regulations, (Chapter 1);
2. Realization of a benchmark on the state of the current state of the art of the tanks in terms of the litters, dimensions, technologies used, the presence of slosh noise baffle solutions, (Chapter 1);
3. Generating 3D models of generic components to simplify the numerical simulation process, (Chapter 4);
4. Designing three innovative technical solutions of wave breakers fixed on the delivery pump module within a fuel tank, (Chapter 4) . For the three technical solutions designed, patent applications have been launched in France and Romania, as well as a European patent extension for one of the solutions. Most of the applications submitted have been formalized in patents.
5. Development of static numerical simulation scenarios for technical wave breaker solutions so as to capture cases of deformability and breaking resistance as close as possible to actual and extreme use (Chapter 5);
6. Transposition of the phenomenon of slosh noise (waves as well as the phenomenon of braking that generates waves) into mathematical modeling that led to the creation of numerical and analytical mathematical models. Their analysis allowed to identify the behavior of the movement of the free surface of the fluid in the studied hypotheses (without integrated wave breaker, respectively with the integrated wave breaker in the fuel tank), (Chapter 6).

7. Identification of the mathematical correlation between the movement of the free surface of the fluid and the level of noise associated with Bernoulli's Integral, (Chapter 6).

8. Development of the computing code in Matlab so as to generate free surfaces related to simulated scenarios with wave-breaker-free fuel tank, (Chapter 6);

9. Development of the computing code in Matlab so as to generate free surfaces related to simulated scenarios with the fuel tank including integrated wave breakers, (Chapter 6);

10. Development of the computing code in Matlab to study the amplitude of waves related to simulated scenarios, (Chapter 6);

11. Develop a test method to reproduce waves in real-world conditions and a scenario for alternatives and test conditions. As presented in the thesis, there is currently no standardized procedure for the reproduction of the slosh noise phenomenon, (Chapter 7);

12. Design and construction of a test bench for the reproduction of waves inside a tank under real running conditions, (Chapter 7);

13. Conducting a set of experiments to measure the noise level produced by the waves generated inside the tank when they collide with the tank walls, (Chapter 7);

14. Develop a methodology for filtering recorded data so as to identify wave noise, which generates the slosh noise effect. Separation of this type of noise from background noise and engine or vehicle braking noise (Chapter 7).

8.3. Dissemination of results

Some of the results obtained from research carried out within the doctoral school were disseminated through:

Publication of four scientific articles:

1. „Study regarding the influence of the fuel tank constructive characteristics on slosh noise effect", Bălaș O., Bălaș R., Doicin C., Applied Mechanics and Materials - Submitted: 2015-09-20 ISSN: 1662-7482, Vol. 834, pp. 22-27 Revised: 2015-10-25 doi: 10.4028/www.scientific.net/AMM.834.22 Accepted: 2015-10-26 © 2016 Trans Tech Publications, Switzerland Online: 2016-04-19

2. „Research and constructive solutions on the reduction of slosh noise", Bălaș O., Bălaș R., Doicin C., IOP Conf. Series: Materials Science and Engineering 161 (2016) 012003 doi:10.1088/1757-899X/161/1/012003-

3. „Statical Analysis of Slosh Noise Baffle", Bălaș O., Bălaș R., Ulmeanu M., Murzac R., Doicin C., Macromolecular Symposia 389(1):1900119, DOI: 10.1002/masy.201900119.

4. „Construction and testing of the wave breaking prototype - slosh noise baffle", Bălaș O., Bălaș R., Murzac R., Ulmeanu M., Doicin C. – being published, UPB Scientific Bulletin, Series D, 2021

Participation in two scientific conferences:

1. ICAMAT 2015 – Advanced Manufacturing Technologies, Romania
2. IMANEE 2016 - Innovative Manufacturing Engineering and Energy Conference, Grecia

A European patent: EP3296136 (A1) — 2018-03-21: Anti-clapping device of a fuel tank of a motor vehicle

Four patents of invention (France & Romania):

1. Patent of invention: FR3060480 (A1) — 2018-06-22. Data deposit : 2016/12/20: Dispositif anti-clapot d'un reservoir de carburant d'un vehicule automobile;
2. Patent of invention: RO132647 (B1) — 30-09-20. Data deposit 2016/12/20: Dispozitiv anti-clipocit pentru un rezervor de carburant al unui autovehicul
3. Patent of invention: FR3061090 (A1) 2018-06-29: Dispositif anti-clapot d'un reservoir de carburant d'un vehicule automobile
4. Patent of invention: FR3055835 (B1) — 2018-08-31: Dispositif anti-clapot d'un reservoir de carburant d'un vehicule automobile

Publication of seven patent applications (three applications in France, three applications in Romania, one European patent application)

1. Patent application: FR3060480 (A1) — 2018-06-22. Deposit Date: 2016/12/20
2. Patent application: RO132647 (A2) — 2018-06-29. Deposit Date 2016.12.20
3. Patent application: FR3061090 (A1) 2018-06-29. Deposit Date: 2016/12/27
4. Patent application: RO132679 (A2) — 2018-06-29. Deposit Date 2016.12.27
5. Patent application: FR3055835 (A1) — 2018-03-16. Deposit Date 12.09.2016
6. Patent application: RO132428 (A2): 30.03.2018. Deposit Date 12.09.2016

8.4. Future research directions

The research presented in the doctoral thesis contributes to the deepening of the conditions for the occurrence of the phenomenon of slosh noise and to the improvement of wave reproduction methods to test various technical solutions. Future research directions may be considered as possible:

1. Research on plastics used in the construction of slosh noise baffles.
2. Research on the design variants of slosh noise baffles in order to make their manufacturing process more efficient
3. Research on the correspondence between noise, frequency and amplitude within the phenomenon of breaking waves inside a tank.
4. Research on mathematical modeling that highlights the correspondence between the movement of the free surface and the noise level generated through Bernoulli's integral
5. Research on the behavior of potential energies through mathematical modeling for tanks that do not present solutions for slosh noise reduction compared to fuel tanks showing on-board baffles.
6. Research on the behavior of kinetic energies through mathematical modeling for tanks that do not present solutions for slosh noise reducing baffles compared to fuel tanks that show on board baffles.

Selective bibliography (extract)

1 [A2M15] Automotive Benchmarking, available at: https://portal.a2mac1.com, accessed on 03.05.2015

2 [ADA16] Adair John, Decision Making and Problem Solving – 3rd revised edition, Editura Kogan Page Ltd, 2016, ISBN: 9780749475611

3 [ALV96] Alvarado Peter J., Steel vs. Plastics: The Competition for Light-Vehicle Fuel Tanks, Journal JOM, 48 (7) (1996), pp. 22-25., available at la https://www.tms.org/pubs/journals/JOM/9607/Alvarado-9607.html

4 [ANS13] ANSYS software User's Guide 15.0, SAS IP., 2013

5 [AUT14] Auto Education – the fuel system, Available at: https://www.autoeducation.com/autoshop101/fuel.htm , accessed on 07.08.14

6 [CHO16] Cho I. H., Kim M.H., Effect of dual porous baffles on sloshing reduction in a swaying rectangular tank, Ocean Engineering 126 (2016)364-373

7 [CHU18] Chu Chia-Ren, Wu Yi-Ru, Wu Tso-Ren, Wang Chung-Yu, Slosh -induced hydrodynamic force in a water tank with multiple baffles, Ocean engineering 167 (2018) 282-292

8 [DEM12] De Man, P. and Van Schaftingen, J. Prediction of Vehicle Fuel Tank Slosh Noise from Component-Level Test Data, SAE Technical Paper 2012-01-0215

9 [DEM18] Demirel Ender, Aral M. Mustafa, Liquid Sloshing Damping in an Accelerated Tank Using a Novel Slot Baffle Design, MDPI Water, 2018, 10, 1565

10 [DEX15] DEX online, available at: http://dexonline.ro/definitie , accesat 13.12.2015

11 [FRA13] Frank Eric, Moon Chris, Rae Jason, Popovich Michael, Optimization of Test Parameters and Analysis Methods for Fuel Tank Slosh Noise, SAE Int. J. Passeng. Cars - Mech. Syst. 6(2):1306-1312, 2013, available at: https://doi.org/10.4271/2013-01-1961

12 [HAL11] Hallez Raphael, McGann Francis, Sibal Stephen D., Fan Li, Radiated Fuel Tank Slosh Noise Simulation, April 2011, DOI: 10.4271/2011-01-0495, available at la: https://www.sae.org/publications/technical-papers/content/2011-01-0495/

13 [HOI04] Hoi Sum IU, W. L. Cleghorn, J. K. Mills, Design and Analysis of Fuel Tank Baffles to Reduce the Noise Generated From Fuel Sloshing," SAE Technical Paper 2004-01-0403, 2004, https://doi.org/10.4271/2004-01-0403

14 [IAC52] Iacob C. „ Introducere matematica in mecanica fluidelor" Editura Academia RPR: An aparitie 1952

15 [IFP16] IFP Training, https://www.ifptraining.com/course

16 [ILI09] Iliescu M., Statistica Aplicata, Edituta Man-Dely, 2009 ISBN 9736-7689-08-9

17 [JAC11] Jacob Pierre, Yohann L'Hermite, Herve Guillerme,Thibaut Prouveur,Laurent Guyotte, Noise reduction baffle and plastic fuel tank comprising such a baffle – Patent WO2010/029103 A1, 2011, aplicant Inergy Automotive systems Research, available at la: https://www63.orbit.com/?locale=fr&ticket=12500403-b249-4262-88de-00c29ddaa297&embedded=false#PatentDocumentPage

18 [LAZ00] Lazar D., Metode matematice in aerodinamica, Editura: Academia Romana, 2000

19 [LIN19] Lin Bing-Ham, Vhen Bang-Fuh, Tsai Chia-Cheng, Method of fundamental solutions on simulating sloshing liquids in a 2D tank, Article in press – Computers and Mathematics with Application, Elsevier Ltd., 2019

20 [LU015] Lu Lin, Jiang Sheng-Chao, Zhao Ming, Tang Guo-Qiang, Two – dimensional viscous numerical simulation of liquid sloshing in rectangular tank with/ without baffles and comparison with potential flow solutions, Ocean Engineering 108 (2015) 662 - 667

21 [LUB15] Lubrifianti Ploiesti, Mase plastice, available at: https://www.lubrifiantiploiesti.ro/mase-plastice/ , accessed on 39.04.2015

22 [MAN15] Manta O., Balas R., Doicin C., Study regarding the influence of the fuel tank constructive characteristics on slosh-noise effect, Applied Mechanics and Materials, Advanced Manufacturing Technologies, Scientific.Net, available at la: https://www.scientific.net/AMM.834.22

23 [MAT16] Mate Vi (base de donnes des materiels) , Norme Gazole FR EN590, available at: https://www.matevi-france.com/fileadmin/user_upload/fichiers_matevi/_PDF/informations_pratiques/Norme-EN-590-2004.pdf, accessed on 23.06.2016

24 [MIC18] Michael E., University of Toronto, Minitab Manual, available at la: http://bcs.whfreeman.com/webpub/statistics/ips6e/Manuals/Student_Minitab_Manual/IPS6e.Mt.St.pdf

25 [MIN20] Minitab, Getting Started with Minitab Statistical Software, available at la: https://www.minitab.com/content/dam/www/en/uploadedfiles/documents/getting-started/MinitabGettingStarted_EN.pdf

26 [PAR10] Park Se-Hyung, Plastic fuel tank comprising a noise reduction baffle and process for manufacturing it – Patent WO2010/023267 A1, 2010, aplicant Inergy Automotive Research, siponibil la: https://www63.orbit.com/?locale=fr&ticket=12500403-b249-4262-88de-00c29ddaa297&embedded=false#PatentDocumentPage

27 [PHA16] Pharea software, Ansys 19.1 Release Notes, available at la: https://www.pharea-software.com/content/uploads/2018/05/Release_Notes_191.pdf , accesat ma 15.06.2016

28 [PLA16] Plastic Omnium – le group, available at la: https://www.plasticomnium.com/fr/industrie/clean-energy-systems-fr/systemes-innovants/systemes-a-carburant-en-plastique.html, accessed on 07.05.2016

29 [PLA19] Plastic Fuel Tanks and Systems for the Automotive Industry – Manufacturer Association, diponibil la: https://www.plasfuelsys.org/index.php?q=plastic-fuel-tank-solutions/they-choose-plastic-fuel-tanks, accessed on 03.05.2019

30 [POG19] Poguluri Sunny Kumar, Cho I.H., Liquid sloshing in a rectangular tank with vertical slotted porous screen: Based on analytical, numerical and experimental approach, Ocean Engineering 189 (2019) 106373

31 [RAM09] Ramsay Thomas, Floating absorber assembly for reduced fuel slosh noise – patent US20090078705 A1, aplicant Honda Motor, 2009, available at la: https://www63.orbit.com/?locale=fr&ticket=12500403-b249-4262-88de-00c29ddaa297&embedded=false#PatentDocumentPage

32 [SAG18] Saghi Hassan, Hashemian Ali, Muti dimensional NURBS model for predicting maximum free surface oscilation in swaying rectangular storage tanks, Computers and Mathematics with Applications 76 (2018) 2496 – 2513

33 [SU016] Su Yan, Liu Z.Y. Numerical model of sloshing in rectangular tank based on Boussinesq type equations, Ocean Engineering 121(2016) 166-173

34 [ULP15] UL Propector – Material Database, available ata la: https://www.ulprospector.com/en/eu, accesata la: 28.03.2015

35 [WAL15] Walbro - engine management and fuel systems, available at la: www.walbro.com , accessed on 05.02.2015

36 [ZOH11] Zohir Benrabah, Francis Thibault, Francis Thibault, Robert DiRaddo, Modeling of Fuel Permeation in Multilayer Automotive Plastic Fuel Tanks, 2011, SAE 2011SAE International Journal of Materials and Manufacturing 4(1):449-459, DOI: 10.4271/2011-01-0248,ResearchGate, available at la: https://www.researchgate.net/publication/314079533 Modeling of Fuel Permeation in Multylayer Automotive Plastic Fuel Tanks